SURFACE ADSORPTION OF CO-POLYMERS

A THESIS SUBMITTED TO

THE GRADUATE SCHOOL OF ENGINEERING AND SCIENCE

OF BİLKENT UNIVERSITY

IN PARTIAL FULFILLMENT OF THE REQUIREMENTS FOR

THE DEGREE OF

MASTER OF SCIENCE

IN

MATERIAL SCIENCE AND NANOTECHNOLOGY

By

Darya Karimpour Khamaneh

August 2022

SURFACE ADSORPTION OF CO-POLYMERS

By Darya Karimpour Khamaneh

August 2022

We certify that we have read this thesis and that in our opinion it is fully adequate, in scope and in quality, as a thesis for the degree of Master of Science.

Aykut Erbaş (Advisor)

Seymur Jahangirov

Ozan Sabahattin Sarıyer

Approved for the Graduate School of Engineering and Science:

Orhan Arıkan
Director of the Graduate school

ABSTRACT

SURFACE ADSORPTION OF CO-POLYMERS

Darya Karimpour Khamaneh

M.S. in Material science and nanotechnology

Advisor: Asst. Prof. Aykut Erbaş

August 2022

Since the Polymer Age was born, researchers have manifested a great interest in investigating polymeric world. Such an enthusiasm arises from polymers' astonishing properties and the sign of their footprint in various places and natural phenomena. Studying the structure of these long molecules of repeating identical units makes a better insight of their mechanisms. Besides, discovering the fact that how polymers enroll in numerous natural events creates a huge opportunity for scientists to mimic their mechanisms in synthetic (human-made) processes or to improve their functions. So far, multitude of models and approaches have been utilized to investigate polymers. Here, we employ molecular dynamics simulations, where we model surface adsorption of co-polymers. The motivation behind this study is to examine if different physical and chemical criteria including initial conditions, chemical structures, and reference frames can have impact on co-polymers' adsorption. Our simulations qualitatively indicate that different co-polymers get adsorbed on the surface. Furthermore, using the data extracted from simulations, we analyze modification of monomers' concentrations while co-polymers get adsorbed on the surface. We, also, quantify changes of brush height, and creation of loops on the surface. Then, by replacing di-block co-polymers (the first type of co-polymers for

our model) with tri-block, random, and alternating co-polymers, also homopolymers, we analyze parameters and reach to distinct patterns for each type of linear co-polymers. In another attempt, we modify strength of interactions to investigate possible impacts of solvent on adsorption process. For the last step, we try to alter the arrangement of co-polymers on the surface, and this time, measure the same parameters and compare results with the previous configuration. We think this study to cascade into more aspects of surface-adsorption of co-polymers, and, in an extensive view, to have implications in the creation of insight into biological phenomena, and/or the biotechnological research and applications.

Keywords: polymers, surface-adsorption, co-polymers, molecular dynamics simulation.

ÖZET

KOPOLIMERLERIN YÜZEY ADSORPSIYONUNU

Darya Karimpour Khamaneh

Malzeme Bilimi ve Nanoteknoloji, Yüksek Lisans

Tez Danışmanı: Dr. Aykut Erbaş

Ağustos 2022

Polimer Çağı doğduğundan beri, araştırmacılar polimerik dünyanın araştırılmasına büyük ilgi gösterdiler. Böyle bir coşku, polimerlerin şaşırtıcı özelliklerinden ve çeşitli yerlerde ve doğal olaylarda ayak izlerinin işaretinden kaynaklanmaktadır. Yinelenen özdeş birimlerden oluşan bu uzun moleküllerin yapısını incelemek, mekanizmalarının daha iyi anlaşılmasını sağlar. Ayrıca, polimerlerin sayısız doğa olayına nasıl dahil olduğunu keşfetmek, bilim adamlarının sentetik (insan yapımı) süreçlerdeki mekanizmalarını taklit etmeleri veya işlevlerini iyileştirmeleri için büyük bir fırsat yaratıyor. Şimdiye kadar, polimerleri araştırmak için çok sayıda model ve yaklaşım kullanılmıştır. Burada, kopolimerlerin yüzey adsorpsiyonunu modellediğimiz moleküler dinamik simülasyonlarını kullanıyoruz. Bu çalışmanın arkasındaki motivasyon, başlangıç koşulları, kimyasal yapılar ve referans çerçeveleri dahil olmak üzere farklı fiziksel ve kimyasal kriterlerin kopolimerlerin adsorpsiyonu üzerinde etkisi olup olmadığını incelemektir. Simülasyonlarımız niteliksel olarak farklı kopolimerlerin yüzeyde adsorbe edildiğini göstermektedir. Ayrıca, simülasyonlardan elde edilen verileri kullanarak, kopolimerler yüzeyde adsorbe olurken monomerlerin konsantrasyonlarının modifikasyonunu analiz ediyoruz. Ayrıca fırça yüksekliğindeki değişiklikleri ve yüzeydeki halka oluşumlarını da ölçüyoruz. Ardından, iki

bloklu kopolimerleri (modelimiz için ilk tip kopolimerler) üç bloklu, rastgele ve alternatif kopolimerlerle, ayrıca homopolimerlerle değiştirerek, parametreleri analiz eder ve her tür için farklı desenlere ulaşırız. lineer kopolimerler. Başka bir girişimde, çözücünün adsorpsiyon işlemi üzerindeki olası etkilerini araştırmak için etkileşimlerin gücünü değiştiriyoruz. Son adım olarak, yüzeydeki kopolimerlerin düzenini değiştirmeye çalışıyoruz ve bu sefer aynı parametreleri ölçüyoruz ve sonuçları önceki konfigürasyonla karşılaştırıyoruz. Bu çalışmanın, kopolimerlerin yüzey adsorpsiyonunun daha fazla yönüne kademeli olarak gireceğini ve kapsamlı bir bakış açısıyla, biyolojik olaylara ve/veya biyoteknolojik araştırma ve uygulamalara ilişkin içgörü yaratılmasında çıkarımlara sahip olacağını düşünüyoruz.

Anahtar sözcükler: polimerler, yüzey adsorpsiyonunu, kopolimerler, moleküler dinamik simülasyonu.

Acknowledgement

First and foremost, I would like to present my appreciation to Dr. Aykut Erbaş for his supervision and guidance throughout this study.

I would like to thank my jury members, Dr. Ozan Sarıyer and Dr. Seymur Jahangirov for their time to evaluate my thesis and for their invaluable feedback.

I would also want to thank the members of the research Lab, Ata Utku Ozkan, Ekrem Mert Bahceci, Zafer Kosar, Muzaffar Rafique, and Ali Göktuğ Attar, who were always welcome my questions, for their helpful and friendly attitudes.

I am thankful to Prof. Ceyhun Bulutay and Prof. Cemal Yalabik for all the pure and unique moments that they gave me in their lectures and for their patience that fulfilled me with the answers to all my questions. Their lectures were the most valuable gifts that I have received in my Master's study.

I am grateful to meet Dr. Seymur Jahangirov and have the opportunity to attend his lectures. He is one of my favorite scientists and I look up to him. Once again, I would like to thank him for his generosity in sharing his knowledge and also for his humility.

I want to thank Noor A. H. Yousuf, Benjamin Edun, Xhulian Lickollari, Ziba Arghiani, Hilal Korkut, Chulhyeong Lee, and all the other classmates, friends, and office mates whom their presence was a huge amount of positive energy to me, and I did not spend time with them as they deserve it.

It is my pleasure to thank Dr. Iqra Munir, Dr.Volkan Aslan, Dr. Nina Sheremet, Dr. Betül Canımkurbey, and Dr. Satish Kumar who were my greatest inspirations in the institute.

I also want to thank the staff of the on-campus housing, the chefs, and the managers of the on-campus cafeterias that brought me to try delicious Turkish dishes and helped

me have a high-quality life during the pandemic (2020-2022).

Finally, I want to express my deepest love to my parents, Taiyebeh and Mohammad, who gave me the gift of incentive to turn my childhood dreams into my golden goals for a transition from being the home's messy princess to a crazy scientist. Also, I am grateful to my lovely twin sister, Donya, our past so-called "hazelnut" and the future pharmacist, for her big heart that taught me courage and kindness. Thank you!

Dedicated to

the strongest woman of my life, Taiyebeh

and the supportive man ever of my life, Mohammad.

Contents

List of Figures

List of Tables

1. Introduction

We are living a life which is constructed of polymers. Anything that we touch in our surroundings, such as glass and plastic products can be made up of polymers, and many of the processes have something to do with these polymeric materials. They are all around us in everyday use, from household items, such as water bottles, toothpaste tubes, clothes, children's toys, and furniture to petroleum products some of which are being used to drive our vehicles[1].

Polymers are long molecules of repeating subunits which are covalently bonded to each other. The special structure polymers have offers them unique properties (e.g., flexibility, and high strength), and allow them to gain tremendous recognition in different fields of science and engineering. This, in turns, makes polymers appreciable in various processes. As an example, polymers have found a special place in new generation of electronic measuring devices such as artificial sensors where they are targeted to imitate natural sense organs[67].

The way that polymers solutions behave in the proximity of a substrate and the properties that they exhibit at the interfaces have captured researchers' curiosity to know more about polymers world. Polymers show different properties when they adsorb to a substrate which accompanies with a change in the composition of a polymer solution. Investigating polymer adsorption (where polymers attach to a surface) provides an opportunity to understand the arrangement and dynamic properties of polymers, also to utilize the obtained knowledge to mimic the process for novel applications. Cell adhesion[68], DNA microarrays[69], and surface patterning[70] are just a few applications of polymer adsorption processes.

In this study, we focus on the adsorption process of copolymers to investigate different aspects of the process. We used computational approaches to simulate the process, and

examine various parameters which determine the outcomes of the adsorption process.

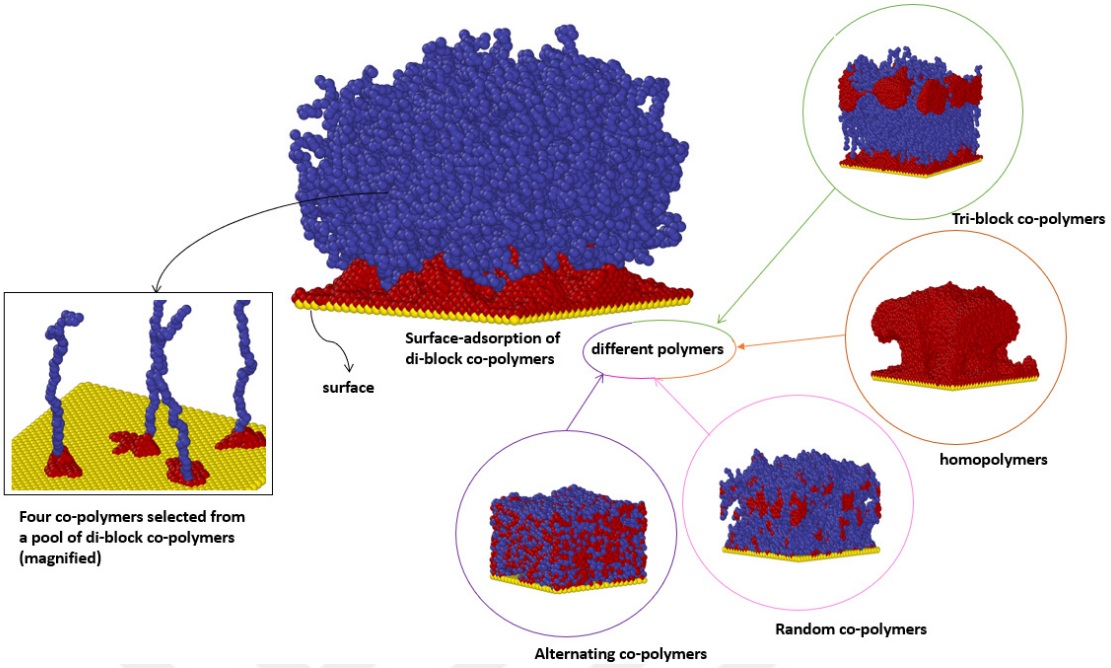

Figure 1.1: An illustration of polymers on a surface containing snapshots of different polymer configurations

The outline of the thesis is in this way: We provide a general view of polymers and the process of adsorption in chapter 2. In chapter 3, we describe the methods that brings the set up and addresses the molecular dynamics simulation as the approach to the study. I, also, discusses the challenges faced during the research. In chapter 4, we concentrate on the parameters whose measurements we seek for during this study. We start with the profile expressing how the pattern of monomers' concentration is near the surface while adsorbing it. Then, we present how the height of co-polymers change during the process. Subsequently, we illustrate that loops are created on the surface and measure the number and length of them. Finally, in chapter 5, we summarize the outcomes and conclude the thesis.

2. Background

One of the magnificence of science is what it explored about the unity of the entire world. Studies demonstrated that the elements making up our bodies, such as carbon and nitrogen atoms, are the ones that exist in the structure of stars in galaxies[2–4]. The discovery of chemical abundance has raised human's curiosity to seek for the connection between stars, cells, and how life began[5,6]. This undeniable fact stating the possibly same origin of the whole universe makes us wonder if our knowledge of materials or natural processes can shed light on similar processes being done in another side of the universe inaccessible to us. Accordingly, efforts to study the matters that exist in various places, first of all, can provide a relatively huge insight into structures and properties of those materials also the processes in which the materials are involved. Secondly, the attempts can increase an opportunity to acquire information about events and places where, due to environmental conditions, far distances, etc., sampling for experimental research is impossible. Thus, through these studies, one can gain knowledge on features of a second phenomenon by the means of studying the according processes and involved substances even though the second is not accessible at the time.

We think polymers can be one of the fascinating substances in this discussion. Polymers have been discovered to be in different constructions from trees[7], bacteria[8,9], and human genes to planetary objects. The solid part of plants, cellulose, is an organic polymer consisting of glucose glycosidically[10,11]. Cellulose is the main component of wood that is synthesized by plants and some bacteria and fungi[12]. This tough fiber not only aids in maintaining plant cell walls stable[13] but also can be counted as a highly strong biomaterial applicable in other constructions. Cellulose synthesized by bacteria have also similar arrangement as plant cellulose. However, they own some differences like water retention properties which is superior in bacteria cellulose leading to its high crystallinity[14]. Bacterial cellulose, as an example of natural polymers, play an integral role in keeping

environmental conditions, such as aerobic condition stable.[1]

Another group of naturally occurring polymers is proteins and DNA. The proteins that we eat, and which a vast domain of our body is made of, are sequences of monomer units named amino acids. Also, DNA is a long molecule constructed of units called nucleotides. These sequence-defined polymers engage in a molecular dance when they are in charge of orchestrating the storage and transfer of genetic information[15]. Their polymeric structures impact on their dramatic functions. Thus, we can see easily that the role of these polymeric materials in the existence of life cannot be neglectable.

A study illustrated that there is a ubiquitous sign of plastic, a polymer on Titan, the largest satellite of Saturn. Scientists claimed that what was discovered on Titan is not pollution from the Earth, so it can be concluded that polymers can be produced and exist in space. Using the Cassini Composite Infrared Spectrometer (CIRS), researchers detected many new molecules including propane, propyne, and propene, all of which are from polymers family, in different layers of Titan's atmosphere[16]. Cassini's projects brought with it the first-ever discovery of polymers outside of Earth and made researchers wonder if polymers may exist everywhere. As this is quoted of Conor Nixon, the leader author of the paper describing finding propene on Titan:

> "This chemical is all around us in everyday life, strung together in long chains to form a plastic called polypropylene. That plastic container at the grocery store with the recycling code 5 on the bottom – that's polypropylene."

Studying structures and functions of these polymers can help to figure out natural processes in which they are involved. For example, determining the topology of plant cellulose microfibrils is significant in understanding the architecture of plant cell walls and the process of cellulose conversion into biofuels occurring in Nature[13, 17–19]. This, in turns, can give a clue to define the native status of inaccessible constructions such as the

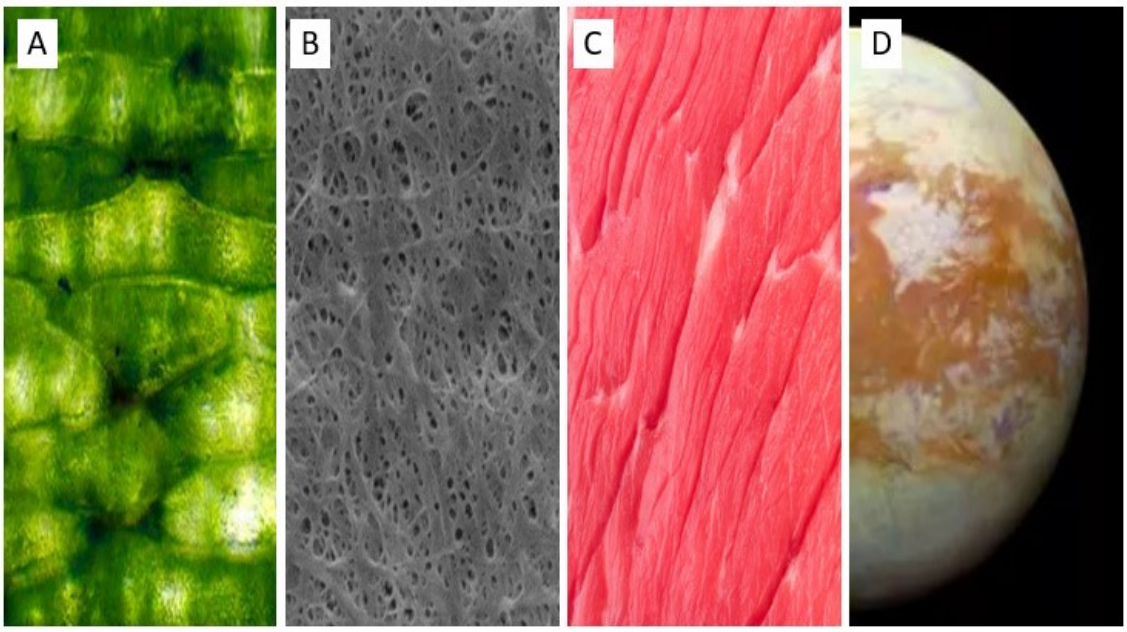

Figure 2.1: Examples of textures where polymers can exist; A. Cell walls of plant leaf, B. SEM image of bacterial cellulose pellicles, C. Texture of raw beef meat, D. Satellite of Saturn

crust of satellites which has this polymeric material inside.

Through this chapter, we overview the history of polymers, structures and properties of polymers and co-polymers. Also, we describe the adsorption process, and the ways that polymers can be modeled.

2.1. Historical review of polymer science

Human history has been always influenced by the availability of primary materials. Transferring from the eras of stone, bronze, and iron, history entered the polymer age in the twentieth century[20].

The initial sign of utilizing polymers in human life goes back to caoutchouc, a type of rubber, that comes from a rubber-tree plant. The large forest tree “Heveea Brasiliensis”, the source of this natural rubber, grew in the southern equatorial region including countries in Africa, Asia, and South America. The name of the material was derived from its use as an eraser, which was first introduced by Priestly in 1770. Humans used this rubber

for many centuries without identifying it as polymer[20–22]. By passing time, they understood more about the nature of this material which resulted in improving the application of it during ages. An example is a discovery occurred in 1839. It was when the rubber heated and, then, treated by other materials like sulfur. The process turned the rubber into an elastic material that was capable of being dissolved in common solvent[23].

The first polymers made by human were actually a modification of original versions of natural polymers. The first man-made polymer, celluloid as it is usually called, was derived from cellulosic materials (natural polymers) and was used for silent-movie film. Then, the application of this synthetic polymer became improved to a fire-proof cover for aircraft wings during the world war[24].

Nowadays, there are many synthetic polymers, which are utilized to create different materials. The use of natural-polymer-based complex molecules has become a great advantage in different fields. A particular example is what gets involved in industry. It has been decades since polymer became the basis of significant goods in industry[25]. They include the production and improvement of food, drugs, and biotechnological items[26]. One of the reasons that turned polymers the central of attention in numerous applications is their capability to self-assemble into nanostructures[27,28]. Various methods and substances have been getting used to synthesize new generation of polymers depending on necessary characteristics (e.g., flexibility, strength, durability). It is worth mentioning that the role of science in this breakthrough is not neglectable though out the history. Among them, we can name the contribution of Hermann Staudinger, a Nobel laureate in chemistry, to polymer science, whose work brought a huge insight into the nature of macromolecules[29]. Besides, Pierre-Gilles de Gennes who won the Nobel in 2000 for developing a theory of phase transition in polymers, and John Fenn, Koichi Tanaka, and Kurt Wüthrich, who developed methods for analyzing biological macromolecules, are a few of researchers whose work have had a great impact on polymer science.

2.2. Microstructure of polymer

Polymers are a particular class of macromolecules whose name emerges from their key feature. The word Polymer built up of two distinct words “poly” and “mer” meaning “many” and “part”. The merge of these two meanings refers to long molecules with a lot of sub-units (monomers), which are a set of repeating chemical units connected to each other like a chain by covalent bonds[24]. The way that monomers attach to each other and the generation of the whole structure of a polymer are determined by a process termed as polymerization.

The procedures through polymerization dictates which monomer units are combined to each other, how they are linked together, and how many units construct the final polymeric structure. The chemical identities of monomers and the type of bonds can influence the physical and chemical properties of a polymeric system[20]. As a result, polymerization not only regulates the appearance of a polymer but also gives rise to specific properties in the polymer. For instance, plant and bacterial cellulose as introduced earlier are chemically identical, meaning the type of monomer units constructing the polymers are the same. On the other hand, the number of units, which also refers as degree of polymerization, is different in these two, ranging from 13000 to 14000 for plant cellulose and 2000 to 6000 for bacterial cellulose[30,31]. Although celluloses synthesized by plants and bacteria have similarities in term of their arrangements and properties, some of their characteristics, such as crystallinity, is far different. Unlike plant cellulose, bacterial cellulose is highly crystalized, which is not independent of the polymer’s degree of polymerization.

Polymer’s microstructure is another deterministic factor in polymer’s properties that shows how monomers are organized along a polymer. Microstructure can be accurately determined by multitude of techniques, such as x ray diffraction, and NMR spectroscopy.

2.3. Fractal polymer conformation- polymer macrostructure

Laws of physics in thermodynamics can describe the dynamical behaviors of polymers and clarifies the reasons behind them. The description is possible when system reaches to an equilibrium state. In this case, the system's macroscopic properties like temperature, pressure, etc. remain fixed. Here, microstates (fluctuations) contribute to a macrostructure of the system whose features became stable. A single macrostructure can be attributed to many different conformations[20].

Conformation is defined as a spatial structure of a system that depends on the relative positions of its components. For a polymer, conformation is specified by the location of its monomers, meaning how monomers are distributed along the polymer after reaching to an equilibrium state. Polymers exhibit various conformations from tight coils to rigid helical chains[32].

Most of the polymer conformations have two special characteristics.

1. self-similarity (being fractal)[33, 34]
2. belonging to universality classes[35]

Fractal is the term used for a system which has items similar to its whole structure. This means if one zooms on a fractal system or a fractal object, she can observe that there would be sections that has exactly the same geometric shape as the whole system. In this case, when the system changes (e.g., growth, distribution, construction), the repetition of the process continues to yield structures categorized at the same fashion at each stage[36]. Fractal dimension is attributed to the system that is the logarithmic proportion of two of its parameters. Fractal systems are characterized by their fractal dimensions. Besides, they are categorized into the classes of systems whose fractal numbers are the same. An example of fractal objects, or self-similar objects, is Koch curve (Table 2.1) which starts

from a straight line, then, by each step of growth, the line gets divided into three equal subunits. The fractal dimension of Koch curve is predicted by the following mathematical formula[37].

$$b = a^d$$
$$d = \frac{\log b}{\log a}$$

Where d is fractal dimension, a and b are the end-to-end distance and number of line sections and fragments, respectively. Division of the magnitude of parameters (shown in Table 2.1) results in $d \approx 1.26$.

Table 2.1: scaling parameters of a Koch curve

n	Koch curve	a	b
1		1	1
2		3	4
3		9	16
4		27	64

The significance of this parameter is that systems within one universality class (due to the fact that they have the same fractal dimension) possess common features. This means if A and B (two randomly chosen systems) are in the same universality class, we can figure out properties of A by the means of studying the properties of B. To illustrate the statement, imagine, after a series of measurements, it is found that fractal dimension of Brownian motion of a molecule in a liquid is the same as fractal dimension of the pattern of a coastline (to be in one universality class). If a scaling property of the coast aimed to be studied; however, measurements are not possible due to restrictions (i.e., tectonic activities, eruptions) researchers can take the pattern of single-molecule motions in a liquid to draw the pattern of the coastline on a map meaning to study a geographical map rather than the real coast.

Like the examples mentioned above, polymers are self-similar objects. When monomers move along polymer chain, it looks like there exist smaller sections which are similar to the entire polymer chain. There is a difference between polymers and the mentioned Various fractal dimension has been measured for different polymers. The reported number for the fractal dimension of ideal linear polymer is $d = 2$.[20]

2.4. Polymeric substances

Polymers can exist in three states of material including liquid, amorphous, and crystalline solid. For example, cellulose (building blocks) is a natural type of solid polymers. Solidity goes back to strong intermolecular forces between polymer units. An important point is that polymers are not though of simply as solids. Their toughness classifies them as amorphous or crystalline. The difference between these two structures is because of the way that polymer units are linked to each other.

Polymeric liquid (e.g., white egg, chewing gum) how quite different dynamical behaviors than the usual liquids. It shows both viscosity and elasticity behavior. For example, a chewing gum shrinks like rubber when it is stretched and then released. On the other hand, it can fill a container like liquid water. This property, termed as viscoelasticity, is one of the key features of polymeric liquids.

2.5. Polymer dynamics

Polymers are structurally flexible. However, monomers are covalently bonded to each other. The reason behind the flexibility is a particular freedom of rotation existing around the bonds[38]. As a result, one can assume that the units constructing a polymer chain adopt random walk conformations[39–41], meaning monomers start diffusing randomly even if there is no net force acting on them. In some polymers (non-ideal polymers), the dynamical behavior is accompanied by a self-avoiding random walk where the polymer

does not tend to intersect itself.

2.6. Co-polymers

Co-polymers are the polymers which are build up two types of monomers. Owing to the complexity of structure and property, co-polymers are grouped into multitudes of categories. The classification of co-polymers consists of molecular architecture (e.g., linear, and branched), order of monomers (e.g., block copolymer, and random copolymer), and material properties (e.g., elastomer, and thermoset)[71].

2.7. Co-polymers at interfaces

Polymers near interfaces reveal different properties in comparison to their bulk properties. The most significant reason for this variety stems from the alteration in the composition of a polymer solution where there is a mixture of polymer and solvent near the interface. Generally, an increase in concentration of polymer solution in the interfacial region is called adsorption.

2.8. Polymer adsorption on surface

As already discussed, adsorption is a process in which a material travel from the first substance and interact with the second. If it gets adsorbed on a surface, meaning it exists in a solvent in the vicinity of a surface, then it will adhere to the surface.

Surface-adsorption of polymers is of fundamental importance in a wide range of technologies, ranging from adhesion to the stabilization and controlled flocculation of colloidal dispersions[72]. Polymer adsorption can occur through physisorption or chemisorption where interactions between the polymer units and the adsorbent are regulated by weak interactions (i.e., van der Waals force) and the chemical valence forces.
Accordingly, solvent is a deterministic factor in the adsorption process in the sense that

interactions between solvent and polymer units govern the flow of the process[73].

2.9. modeling polymers

Scientists develop models and formulate testable hypotheses to understand polymers' arrangement and dynamical behavior in solution, based on the principles of polymer physics. Multitudes of strategies are utilized for modeling polymers from MD, to machine leaning methods. In modeling polymers two factors play a key role in simulations.

One is the features chosen for monomer units which is proportional to most real properties of polymers, and the other is the interactions which defines how monomer units are attached to each other, and how the interactions between non-bonded components are. Based upon success in modeling processes like surface adsorption of co-polymers with molecule dynamics simulations[74], plus, the clarity that these simulations follow, researchers opt to utilize such an approach to predict the structure.

Scientists develop models and formulate testable hypotheses to understand their arrangement and dynamical behavior in solution, based on the principles of polymer physics.

3. Methodology

3.1. Configuration

3.1.1 Surface design

To begin modeling surface-adsorption of co-polymers, firstly, we required to design a surface. To do so, we considered a group of beads of identical spheres that constructed a square layer. We chose a common crystal structure, FCC (face-centered cubic),to arrange the beads next to each other. The motivation behind the selection of FCC structure for the surface is that the number of nearest neighbor atoms in this lattice structure is the maximum (the coordination number is 12)[42]. Thus, we can make sure there is the least empty space in the surface. The thickness of the square surface (as shown in Figure3.1 A.) is equal to diameter of a single bead which is $r = 0.5\sigma(\approx 1.7 \text{ nm})$, and the total number of beads constructing the surface is 1681.

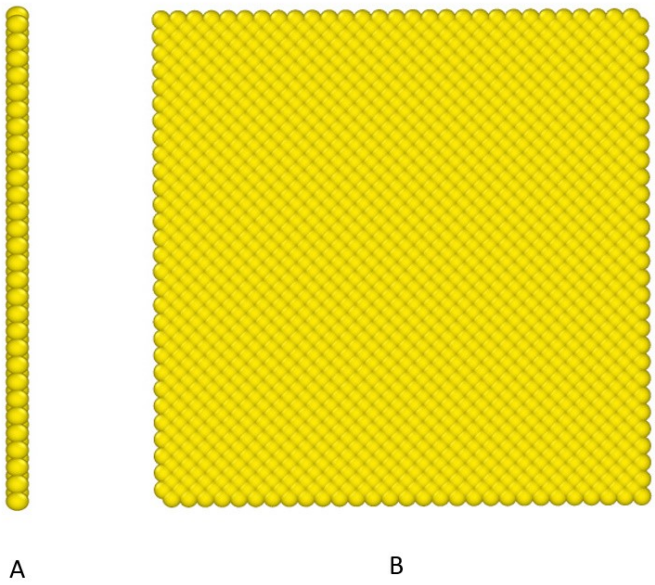

Figure 3.1: A representative snapshot of the surface A) A perspective view of the surface showing the thickness it, B) A side view of the surface showing the surface area

3.1.2 Di-block co-polymers design

As described in Chapter 2, there are multitudes of architectures for co-polymers. We confined them to linear co-polymers for our model because we wanted to consider possibly the simplest and the most symmetric geometric shapes ignoring complex structures. Instead, we aimed to examine other factors influencing the adsorption process, which will be explained further. It is worth mentioning that linear co-polymers are applicable for modeling biological systems, as they were utilized in former works[43]. Thus, our model can have implications in biological studies. Accordingly, we defined two groups of beads (all the beads are identical spheres), which construct di-block co-polymers. The only difference that these two groups of beads have is the type of them. In each co-polymer, the first half of beads are type-1, and the other half are type-2 which results in a di-block co-polymer. We defined the positions of beads in the way that co-polymers get placed vertically near the surface (perpendicular to the area of the surface). A data file including the information of all the beads (i.e., number, type, position in 3D space) was prepared. We defined bonds between any two neighboring beads in each linear co-polymer whose information was described in the data file (bonds will be explained in more details in further sections). There are totally 256 co-polymer chains on the surface, each of which consists of 100 beads.

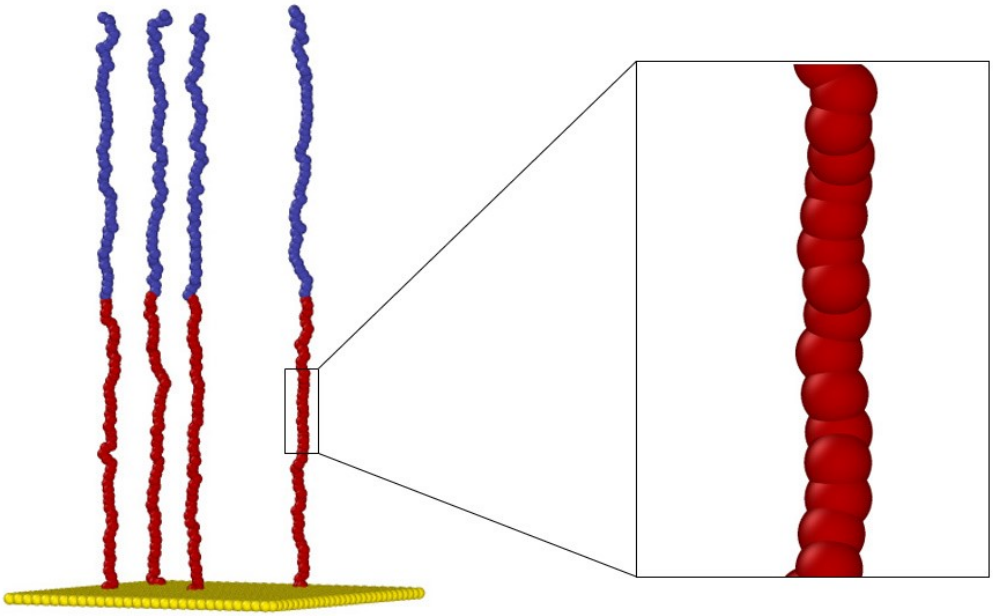

Figure 3.2: A snapshot of four co-polymer chains arranged on the surface; A piece of one of the chains has been magnified to show the arrangement of beads along the chain.

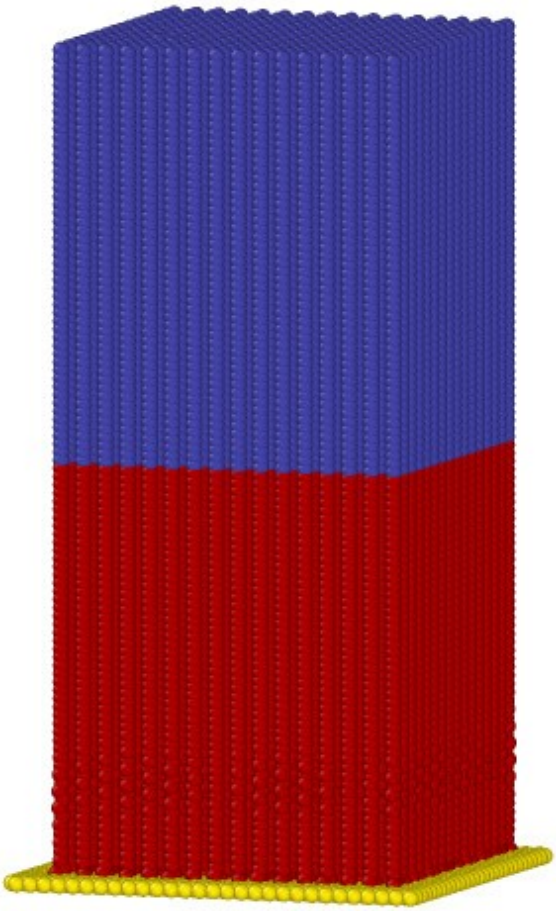

Figure 3.3: A snapshot of the initial configuration of the model

3.1.3 Replacing di-block co-polymers with other linear co-polymers

Beside di-block co-polymers, we are also interested in other polymer architectures. To add co-polymer chains with different order of monomers, we utilized a quantity introduced in former studies. This parameter attributes an identity to every type of co-polymers, which indicates how beads constructing a chain statistically correlate with each other. Firstly, the statistics governing the co-polymers' identities (termed as chemical identity) were defined. We predicted the identities chase Markov Chain Statistics model[39]. In this model, the propagation of chemical identities along a chain is regulated by the propagators $\rho_{\alpha_2}^{\alpha_1}$, which offers the probability that if a bead (in our model) has chemical identity α_1 that the next bead will have chemical identity α_2. Then, for a two-state system like co-polymers, the degree of chemical correlation along a co-polymer chain is governed by the following equation[44].

$$\lambda = \rho_A^A + \rho_B^B - 1$$

where ρ_A^A gives the probability of having a type-1 for the next bead if the first bead is type-1, and ρ_B^B shows the probability of having a bead with type-2 when the previous bead is also type-2.

Accordingly, for a di-block co-polymer, the degree of chemical correlation is $\lambda = 0$ since ρ_A^A and ρ_B^B are equal to 0.5 for a chain with a half containing type-1 beads and the other half consisting of type-2 beads. Moreover, if there is a random co-polymer, meaning the order of beads along the chain does not obey any pattern and is chosen randomly, then for ρ_A^A and ρ_B^B there would be either of these two cases; ρ_A^A is one and ρ_B^B is zero, or ρ_A^A is zero and ρ_B^B is one. This gives the degree of chemical correlation $\lambda = 0$. For the model of tri-block co-polymers, if the starting bead is type-1, then $\rho_A^A = 2/3$ (two third of the chain would have type-1 beads), and if the bead is type-2, then again there would be $\rho_B^B = 2/3$. This results in the degree of chemical correlation $\lambda = 1/3$. If all the beads

along a polymer chain are of the same type, then ρ_A^A and rho_B^B are one, which ends up to $\lambda = 1$. This means the degree of chemical correlation for homopolymers is $\lambda = 1$. And finally, if there are not any two beads with the same type next to other along the chain, then ρ_A^A and ρ_B^B are both equal to zero, which results in the degree of correlation $\lambda = -1$ for alternating co-polymers. In this way, we substituted di-block co-polymers with the other four linear hains (shown in Figure 3.4), and tested how degree of chemical correlation affects results.

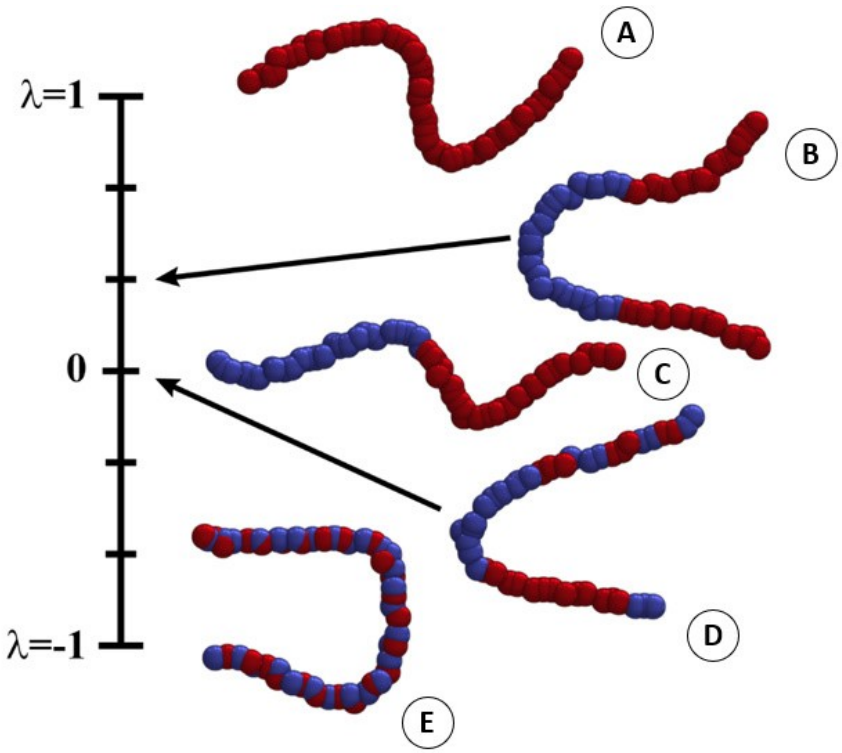

Figure 3.4: An illustration of five types of co-polymers according to the chemical correlation parameter; A) homopolymer, B) Tri-block co-polymer, C) Di-block co-polymer, D) Alternating co-polymer, E) Random co-polymer

3.1.4 Co-polymers relaxation

Although previously introduced model (figure 3.3) satisfied the condition for surface-adsorption of co-polymers, co-polymer chains need to be relaxed before the beginning of the process. This means, instead of having well-organized straight lines of co-polymer chains, we need to have the beads giggling along the chains. As a result, we need to relax

the co-polymers.

To do so, we ran simulations with initial configuration by adding a term of interactions between type-1 beads and the beads of surface, also having repulsions between other components of the system. Attractions and repulsions were appointed via fixing interaction distance threshold $r = 2.5\sigma$ and $r = 1.122\sigma$ distances below, respectively, where interactions start taking over according to Lennard-Jones potential, which is governed by the following equation[45,46].

$$4\epsilon\left[\left(\frac{\sigma}{r}\right)^{12} - \left(\frac{\sigma}{r}\right)^{6}\right]$$

Using 2×10^5 steps and a timestep of $\Delta t = 0.001\tau$, we could make the initial configuration of co-polymers relax enough to start the main process. The chains are no longer fully straight at the end of relaxation time. (Figure 3.5)

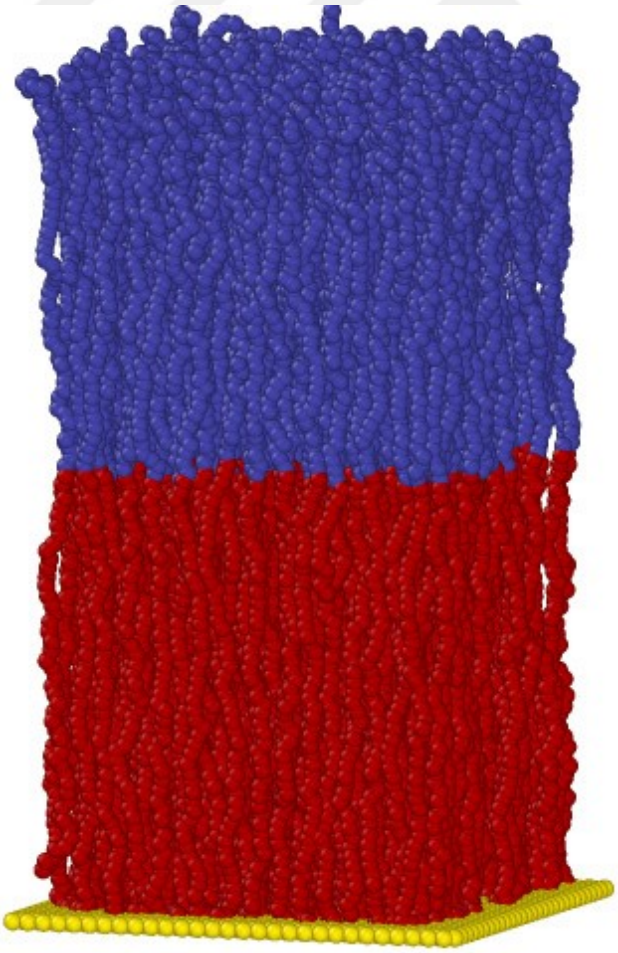

Figure 3.5: A snapshot of the relaxed co-polymers

3.1.5 After relaxing the co-polymers

When the relaxation time came to end, we would have a new data file including new positions of all the beads. Using the data file, we ran the second part of simulations which we expected to lead to the surface-adsorption process. For this section, we added another term of interactions which is attractions between type-1 beads. Therefore, each type-1 not only gets attracted by surface beads but also has interaction with other type-1 beads. This short-term interaction is also governed by Lennard-Jones potential with the interaction distance threshold $r = 2.5\sigma$.

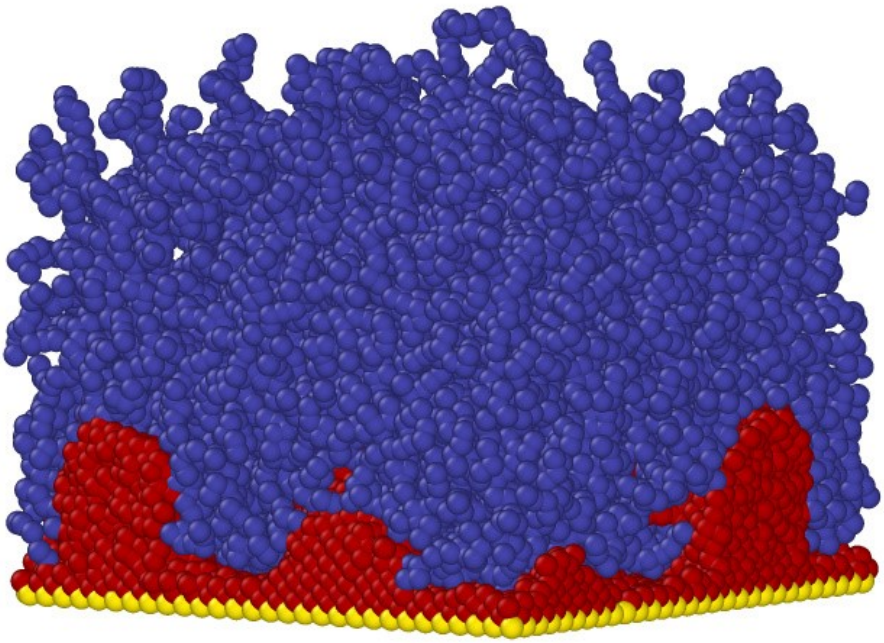

Figure 3.6: A snapshot of the configuration after the relaxation time

3.2. Analyzing simulation file

3.2.1 Concentration profile

Following our simulations' runs, we aimed to analyze the simulation results to investigate the adsorption process of co-polymers. The output of each of our simulations is a dump

file which contains all the positions of all the beads in three-dimensional space at each simulation time. Using visualization tools such as OVITO and VMD, we can access the visual inspection of dump files. These 3D visualization softwares allow the user to watch simulations as movies. Therefore, each frame of the video reflects a specific timestep, and the evolution of the system can be analyzed.

Even though this approach gives a relatively comprehensive view of simulations, it only provides the qualitative aspects of the process. An appropriate approach to study and analyze the process quantitatively is utilizing computational tools. Reading a dump file (containing the positions of all the beads), our program separates the information of each bead into 2D arrays where one dimension contains the bead IDs and the other contains their types and positions. Then, the program counts the beads within specific distances above the surface. Finally, patterns of beads' concentration above the surface are plotted.

3.2.2 Curve fitting the concentration profile graphs

Among beads concentration profile graphs, we saw gaussian and exponentially decays. Thus, we decided to fit an appropriate graph for each data. Accordingly, we used the Python SciPy library optimize module for the fitting, and derive the coefficients of gaussian and exponential distribution functions.

3.2.3 Calculating volume fraction

Volume fraction refers to the occupied volume of polymers per unit volume of solution or bulk. We calculated volume fraction of each configuration of the following equation.

$$\varphi = \frac{n \times v}{V}$$

Where φ, a unitless quantity, is the volume of fraction, n is the number of beads of polymers, v and V are the volume of a bead and solution (or bulk), respectively.

3.2.4 Measuring height of brushes

Polymer brushes forms when polymers are tied at one end to a substrate. These polymeric assemblies are applicable in different fields like nanolithography, drug delivery, and so on.

Our program first reads the dump file similar to the concentration profile section. Then, it calculates the vertical distance between the first and the last type-2 beads of each chain. Next, it averages this quantity for all the chains in each timestep. Finally, plot the graph of the calculated height within time interval. Accordingly, the plots show the changes of co-polymers brush through the simulated process.

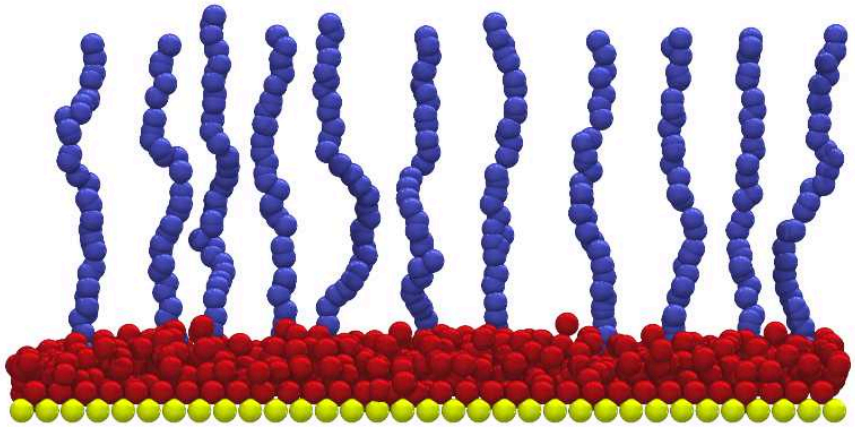

Figure 3.7: A scheme representing co-polymer brushes

3.2.5 Quantifying loop formations

Polymer looping absorbed a significant attention particularly in biological sciences. Loops appear in biopolymers where they have a great impact on biological processes. For example, gene regulation in living cells highly dependent on DNA (a long bio-polymer) looping. The interaction between DNA-bond protein and a target site on the same DNA takes place more frequently on loop regions which results in accelerated enzyme reaction rates[47–49]. Moreover, the looping of proteins, which are the polymers of amino acids, plays a central role in protein folding. The places where the loops occur are the binding sites of other molecules[50].

We aimed to look for possible loops formed on the surface and characterize their sizes. The approaches began with reading the output file by our program. Starting from the first bead in data file, our program finds the first index of beads with the vertical distance of $d \leq 0.5\sigma$ from the surface. Then, the program counts the number of beads whose vertical distance from the surface is $d > 0.5\sigma$. The procedure will continue till the counted bead has $d \leq 0.5\sigma$. The number of counted beads is the size of the corresponding loop.

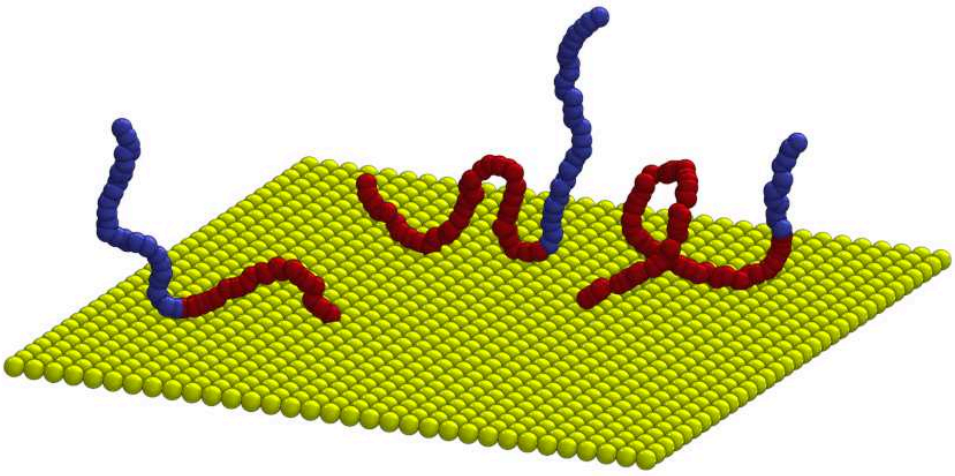

Figure 3.8: A scheme representing loop formation on the surface

3.2.6 Finding knots

Knots are complex structures that can be created in entangled systems. Like polymer looping, knotting may occur in polymers such as folded proteins[51]. Molecular chains fold into proteins and genes like the way that a rope gets tied into a knot.

We tried to search for possible knots along the co-polymer chains of our simulations. To do so, we considered the simplest knot termed as Trefoil knot (Figure 3.9). Our program plots the coordinates of the beads of each chain separately. Then, the program searches for two conditions. The first is to find any two pairs of beads along a single chain whose z-components are approximately the same (repeated for other components). Second, if the first bead of the first pair has a larger distance from the origin of coordinate system, then the first bead of the second pair should have a smaller distance of the origin. Meeting both conditions is the sign of the existence of a knot along the chain. Unfortunately, we did not find any beads satisfying the condition. The defect of our approach may be due to projecting a knot in a particular direction. Another idea could be that the length of co-polymer chains did not fulfill the situation of knot formation.

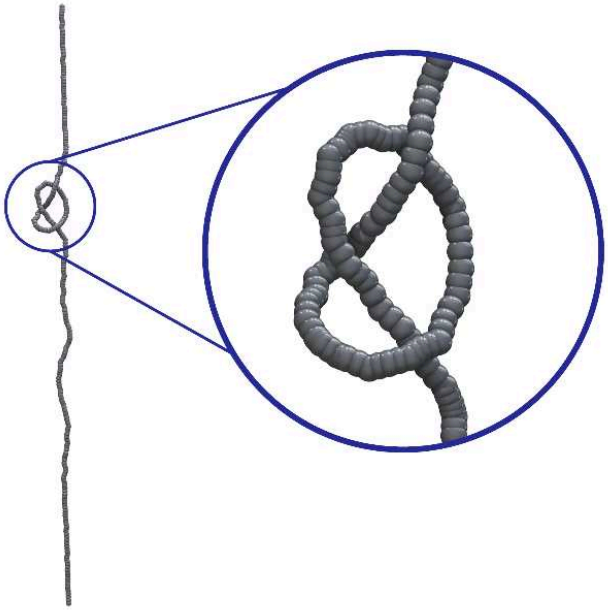

Figure 3.9: A scheme representing a Trefoil knot along a chain

3.3. Simulation model

To simulate surface adsorption of co-polymers, we employed bead spring model, first introduced by Grest and co-workers[52–56], for co-polymers in implicit solvent conditions. Our system consists of a square shaped surface and 256 identical linear co-polymers. Each co-polymer consists of 100 monomer units, which are counted as beads in the model. The co-polymers are formed by identical beads which are spheres with the mass of $m = 1$ in Lennard Jones units and the size of $r = 0.5\sigma(\approx 1.7$ **nm**$)$. There is a fixed surface located near the co-polymers. It is made of a layer of beads with the same size as the co-polymers', and the width and the length of it are $40\sigma(\approx 136$**nm**$)$. Also, it is 0.5σ high which is equal to the diameter of a single bead. A cubic simulation box is considered with periodic boundary condition and with the dimension of $46 \times 46 \times 101\sigma^3$.

Co-polymers are placed vertically on the surface. The nearest bead to the surface is 2σ above the surface, and neighboring beads in every co-polymer chain are 0.86σ distant from each other.

3.3.1 non-bonded interactions

In our system, interactions between components get divided into two categories, non-bonded interactions and bonded interactions. Non-bonded interactions, which are derived by a composite potential formulated by Steinhauser[57], operate between all pairs of beads. For this term, we employed shifted Lennard Jones potential[58]. The intended LJ potential is governed by

$$V(r) = \begin{cases} 5\,u\left[\left(\frac{\sigma}{r}\right)^{12} - \left(\frac{\sigma}{r}\right)^{6} + v_s\right] & r \leq r_c \\ 0 & r > r_c \end{cases}$$

We defined interactions between the first 50 beads of every co-polymer nearest to the surface and the surface beads as attractive interactions. Here, cut-off distance is set to

$= 2.5\sigma$, and shift factor is $v = 0$. The interactions operate between these 50 beads, named as type-1, is also attractions.

On the other hand, for the second 50 beads of each co-polymer, we set the cut-off distance to $_c = 2^{1/6}\sigma$, and the shift factor to $v = 1/4$ for creating repulsive interaction conditions. These beads are referred to type-2 beads. Besides, beads constructing the layered surface are tagged as type-3. While the type-3 group (surface beads) attract or repulse type-1 and type-2 beads, we need them to stay in their primary position. As a result, we excluded the forces acting on type-3 beads to have the surface unmodified.

3.3.2 Covalent bonds

In our model, 100 beads forming every co-polymer are connected to each other using a non-linear finitely extensible FENE potential[52]. The potential is regulated by the following equation.

$$V_{FENE}(r) = \frac{1}{2}kR_0{}^2 \ln\left(1 - \frac{r^2}{R_0{}^2}\right)$$

Here k is a spring constant, R0 is the maximum possible bead-bead separation, and r is the bond distance. We took $R_0 = 1.5\sigma$, and $k = 30\varepsilon/\sigma^2$, where σ and ε are distance and energy parameters, respectively. The above equation provides the bond distance $b = \sigma$.

3.3.3 Angles

The signature characteristic of polymers is flexibility. To add this property to the co-polymers of our model, we employed another term of interactions which is created by a harmonic bending potential. The bending potential makes beads have more degrees of freedom modifying the angle between three consecutive beads of a co-polymer chain while moving around. The bending potential is formulated by the following equation to

model semi-flexibility of co-polymers.

$$V = \frac{1}{2} k_\theta \left(\theta - \theta_0\right)^2$$

Where the spring constant is $k_\theta = 2\varepsilon/\text{rad}^2$, and the initial angle between three consecutive beads is $\theta_0 = \pi$.

We carried out all the simulations using the LAMMPS MD package[59]. The simulation boxes are maintained at constant temperature constant volume ... .

We used OVITO and VMD[60,61] for visualizations, also Python NumPy, Python Pandas, and Matplotlib packages[62–64] for analyzing data and measuring parameters.

3.3.4 Thermodynamic stabilization

Using statistical ensembles, we set the thermodynamic condition of the systems to have a fixed absolute temperature. we kept the temperature constant via a thermostat coefficient of $\gamma = 0.5\tau^{-1}$ with Langevin thermostat style.

3.3.5 An alternative model for co-polymers

One of the fascinating portions of solving problems from physics perspective is to view systems from various frames of reference[65,66]. The aim is to compare possible results derived from each reference and compare them to find out how comparable they are.

Addressing a question requires us to know two properties of components involved in the question, position and momentum. The first characteristics allows us to discover locations of particles, and the second lets us know what instant velocities of the particles are. Accordingly, we will be able to find the track of particles by the use of mathematical expressions. Using mathematical equations which formulates the dynamics of particles,

we can study behavior of the corresponding system. Accordingly, position and momentum are the two criteria enough to know revolution of a dynamic system. Following the pattern of momentum (mass times velocity) is the key to understand if any external forces are acting on the system. Revolution of a system can be described by interactions (external forces) between any pairs of components.

A reference frame is necessary to begin solving a question in physics. In this way, factors like positions, velocities, and forces are defined regarding the reference frame called initial reference frame. Substituting the initial frame with other frames may alter the factors; therefore, it can change the outcomes describing the behavior of the physical system. However what science expects to occur is that consequences stay the same while solving the question from different frames' point of view. An example for this claim is the motion of a ball thrown in the air vertically. Taking the ground, the ball, or another planet moving in terms of the earth as a reference frame results in non-identical outcomes.

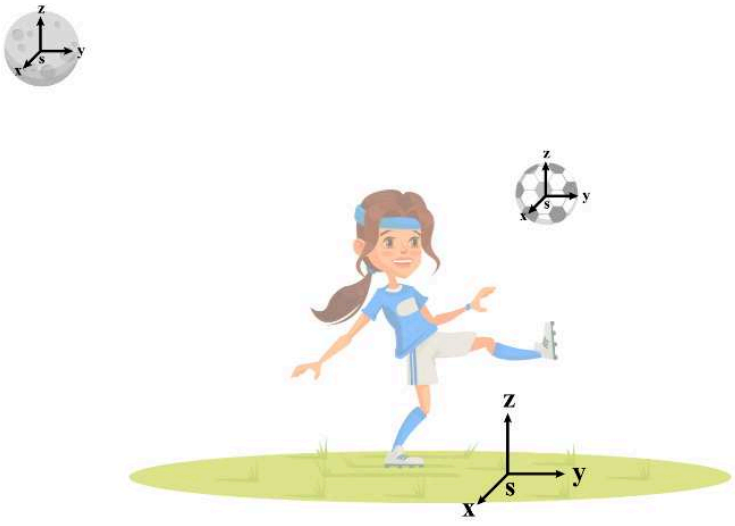

Figure 3.10: An illustration showing various reference frames

Rather than selecting a reference frame for a system, initial conditions is also decisive to determine final state of a system through its revolution. We attempted to consider two initial conditions, one of which was described above, and analyze and compare the results with each other.

We opted for horizontal co-polymers placed on the surface, whose monomers are randomly distributed along the chain. Here we started with locating the first bead (monomer) on the surface, then multiplied the position of the bead with tan(θ), where $0 \leq \theta \leq \pi$ is the angle selected randomly for the next bead. Each co-polymer consists of 100 beads just like our previous model. When co-polymers filled a layer of surface, we added new chains on top of them and constructed a layered structure of co-polymers near the surface. There are approximately 17-20 co-polymer chains in every layer, and the number of layers is 4. Setting up chains in the model caused some restrictions regarding long bond distances and chains movements next to each other; thus, we chose the total number of co-polymers as 70 which is less than the number of chains in our previous model. Accordingly, we reduced the size of the surface to $52 \times 41 \times 101\sigma^3$ to make the proportion between number of chains and surface area approximately the same in both of our models.

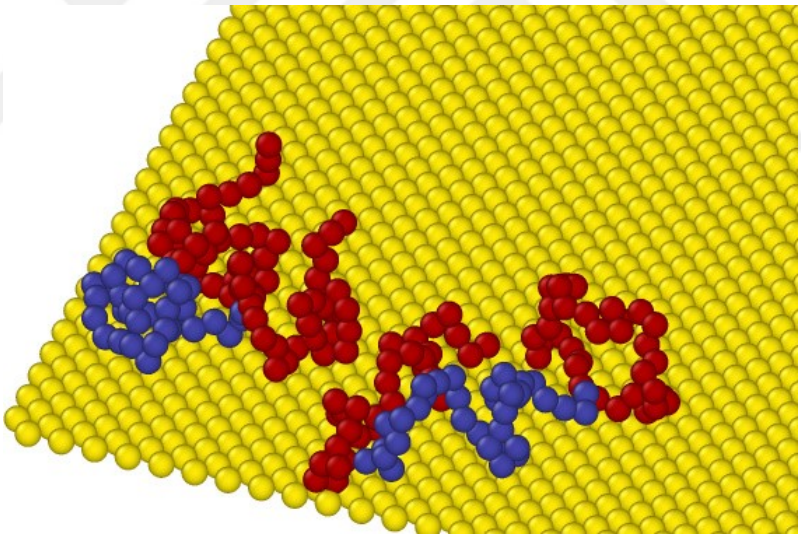

Figure 3.11: A snapshot showing two co-polymers are distributed randomly on the surface

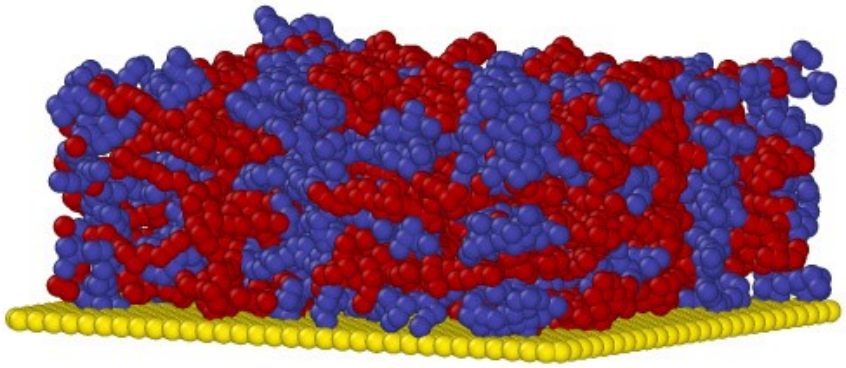

Figure 3.12: A snapshot showing the configuration of the second model

4. Results and discussion

In this chapter, simulating achievements for surface-adsorption of copolymers are qualitatively shown. Simultaneously, intended parameters are measured for every configuration using the data extracted from simulations. Moreover, the quantitative results are utilized to characterize specific configurations based on multitude of factors (e.g., strength of interaction, co-polymer population). Furthermore, it is tested how co-polymers arrangement and chemical correlation of co-polymers influence the adsorption process, and parameters are quantized for each of the systems.

4.1. Surface-adsorption of di-block co-polymers

Our primary goal is to simulate and observe the adsorption of di-block co-polymers on a surface. As previously described, in our initial configuration, there are 256 vertical identical di-block co-polymers which are linear chains consisting of a hundred of beads. Half of each chain contains type-1 beads (illustrated in red color), and the other half are built of type-2 beads (illustrated in blue colored). Compared to blue beads, red beads are in the less distance from the surface. Firstly, co-polymers are relaxed for 2×10^5 steps with a timestep of $\Delta t = 0.001\tau$, where surface attracts red beads (type-1) with the weekly attraction interaction $u_{sb} = 5kT$, and the interactions between the other elements are repulsive $u_{bb} = u_{sb} = 2kT$. Then, attractions between red beads, $u_{sb} = 5kT$ are added to the interactions, and the simulated process lasts for 5×10^6 steps with $\Delta t = 0.002\tau$ timestep.

Our MD simulations (snapshot in Figure 4.1) illustrates how co-polymers get attracted on the surface, where red beds come to the vicinity of the surface and some of them attach to it, also the height of blue beads decrease and they get distributed near the surface on top of a thick layer of blue beads. Even though we cannot claim that the

simulations present the adsorption process perfectly, we can qualitatively observe several features.

The area of the surface is filled with red beads linked to it, and the other red beads gather on this layer making a red huge mass on the surface. Although initially the square surface and the co-polymer chains build a symmetrical geometry, the aggregation of red beads on the surface does not contribute to a 3D cube-like shape. It is more like half of a cylinder on middle of the surface (Figure 4.1). Blue beads pile up on top of the red area, and the ones farther from the surface are more vibrant shaking around.

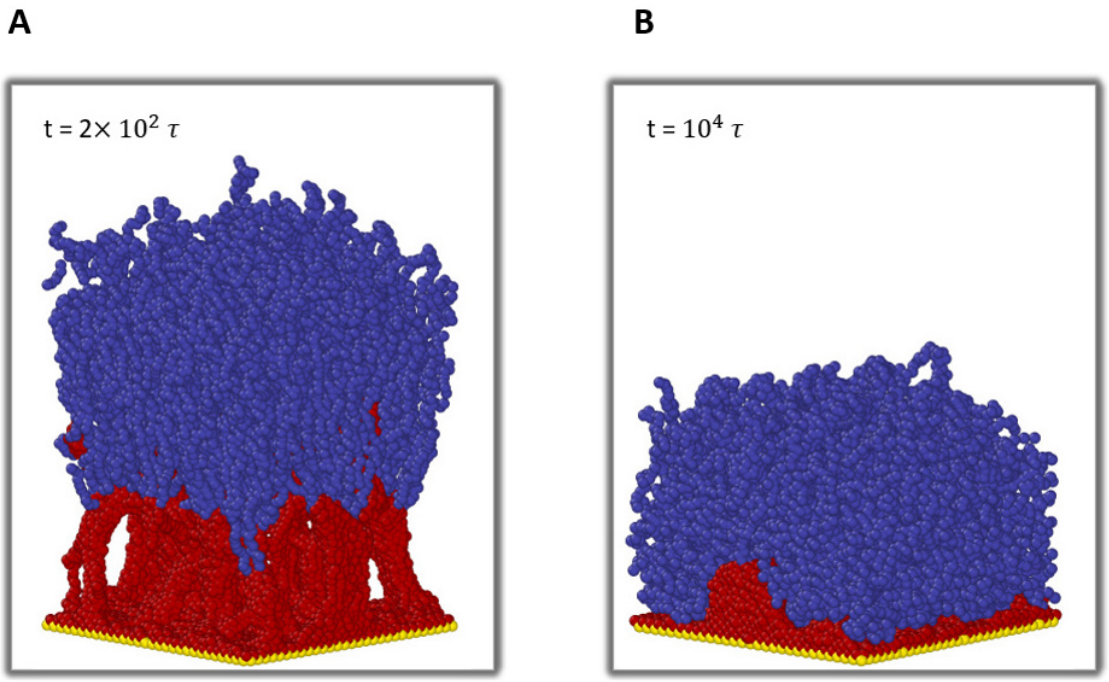

Figure 4.1: Snapshots of the simulation; A) a frame of the simulation after the relaxation time, B) the last frame of the simulation

To analyze how particles are distributed above the surface, we wanted to plot bead concentration profile which shows the density of beads with respect to their vertical distance from the surface.

Figure 4.2 is the plot showing the distribution of beads including red and blue beads above the surface. To obtain a solid view and to quantify the graphs, we plot the functions

corresponding to the number of red beads and the number of blue beads (Figure 4.3). Moreover, we calculated the mathematical equations of each function.

The green graph representing the total number of di-block co-polymers with respect to their vertical distance from the surface indicates some fluctuations in the distribution pattern. This can accord with the natural behavior of particles, meaning the existence of fluctuations before reaching to stable states.

The exponential $(a \times \exp(-b \times x) + c)$ and gaussian $(a \times \exp(-(x - x_0)^2/(2 \times \sigma^2))$ functions obey the equations of $324.25 \times \exp(-0.08 \times x) - 21.07$, and $114.67 \times \exp(-(x - 18.68)^2/(2 \times 9.35^2))$, respectively.

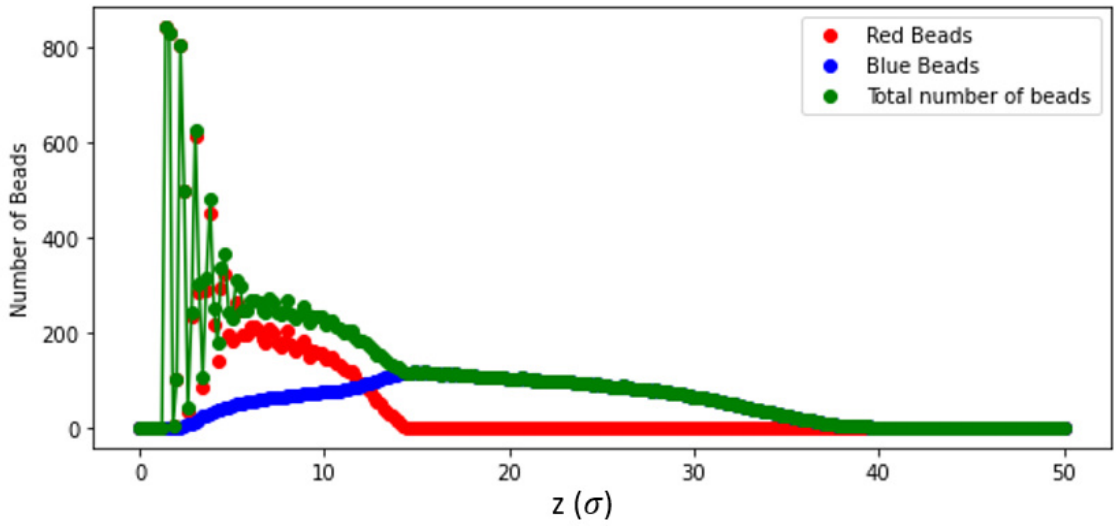

Figure 4.2: Number of beads with respect to their z-distance from the surface. Here, the red graph, the blue graph, and the green graph represent the number of red beads, the blue beads, and the total number of beads (red and blue beads), respectively.

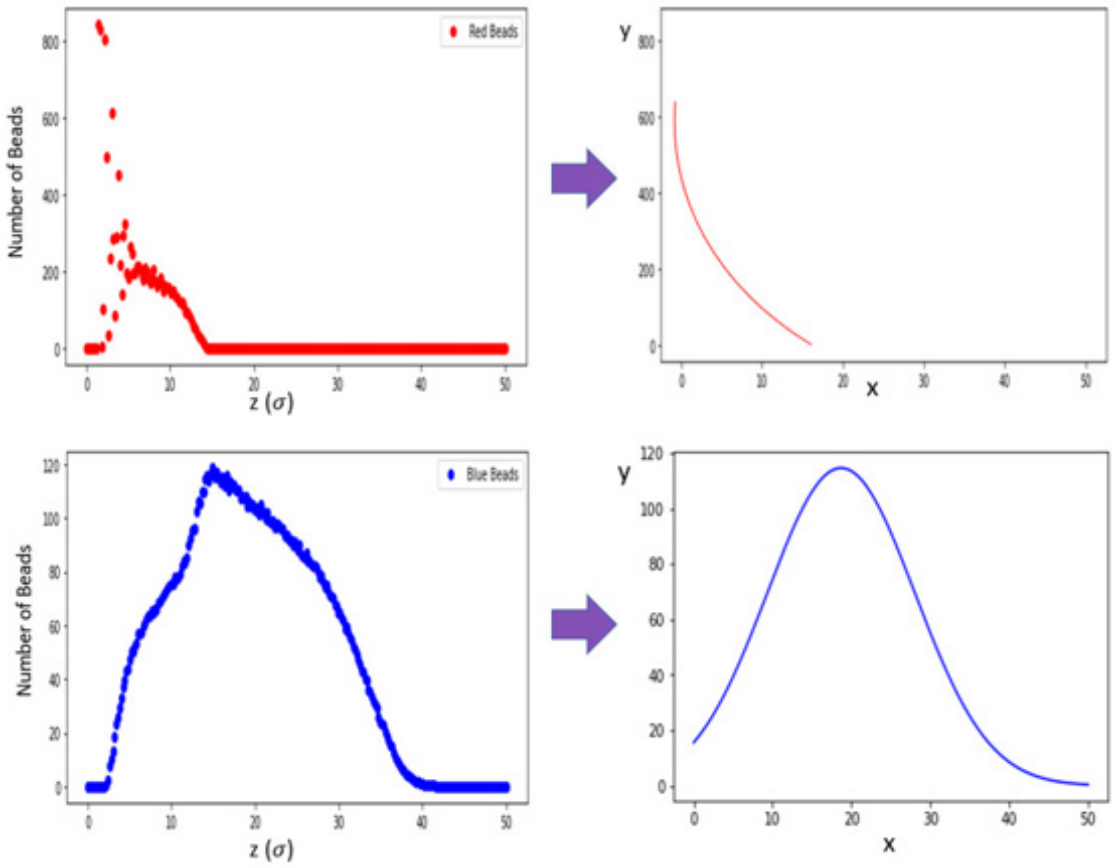

Figure 4.3: plots showing the number of red beads and blue beads above the surface, the curves fitted on the pattern of beads are exponential and gaussian functions for red and blue beads, respectively.

4.2. The effect of strength of interactions on adsorption process

As previously mentioned, we defined weak interactions between any non-bonded beads. In this section, we wanted to modify the strength of these interactions to examine how they influence the process. Accordingly, we changed $u_{sb} = 5\,kT$, which is attractions between red beads and surface beads, to $u_{sb} = 3\,kT$, $u_{sb} = 10\,kT$, and $u_{sb} = 15\,kT$. Then, for each of the new systems, we kept the repulsions between other beads the same as the previous section $u_{bb} = u_{sb} = 2\,kT$.

When the attractions change to 3KT, co-polymers do not get closer to the surface, but they go up distributed at higher distances from the surface (Figure 4.4). Therefore, the interactions are not strong enough to accumulate beads near the surface and to adsorb

the co-polymers on the surface. For configurations with the strength of attractions of 10KT, red beads gather on the surface and blue beads get closer to the surface distributed on top of the red beads (Figure 4.5).

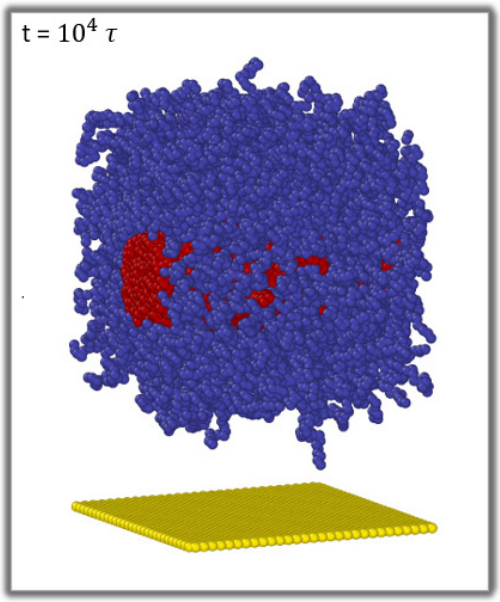

Figure 4.4: Snapshot of the simulation. The attraction between surface and red beads is $u = 3KT$, and co-polymers are not adsorbed on the surface. Red beads attract each other with the strength interaction of $u = 3KT$ and make a red cylinder above the surface, and blue beads, which repulse each other with the strength of interaction $u = 2KT$, gather around the red cylindrical shape.

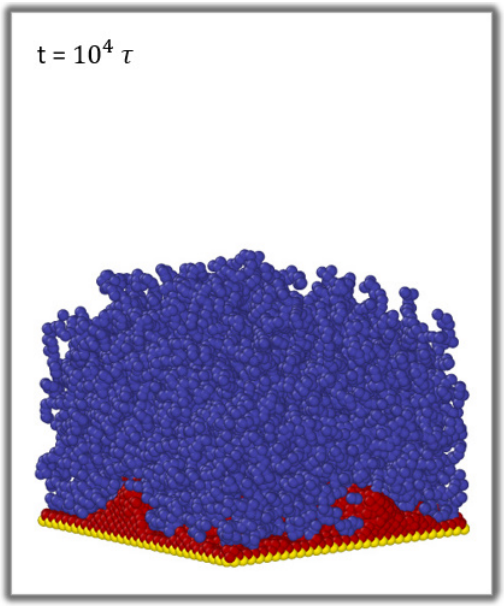

Figure 4.5: Snapshot of simulation, the last frame of the simulation where the strength of attractions between red beads and the surface, and between red beads with themselves are $u = 10KT$, and blue beads repulse each other with the strength of interaction $u = 2KT$.

We analyzed the concentration profile of beads in this system and obtain the patterns of beads distribution. In this system, the concentration of red beads is denser than the previous one near the surface, meaning the increased strength of attractions (here it is doubled) leads to the more concentration of beads near the surface.

The exponential function corresponding to red beads is $329.38 \times \exp(-0.09 \times x) - 20.58$, and the equation represented the distribution of blue beads is $116.92 \times \exp(-(x - 19.06)^2/(2 \times 9.14^2))$.

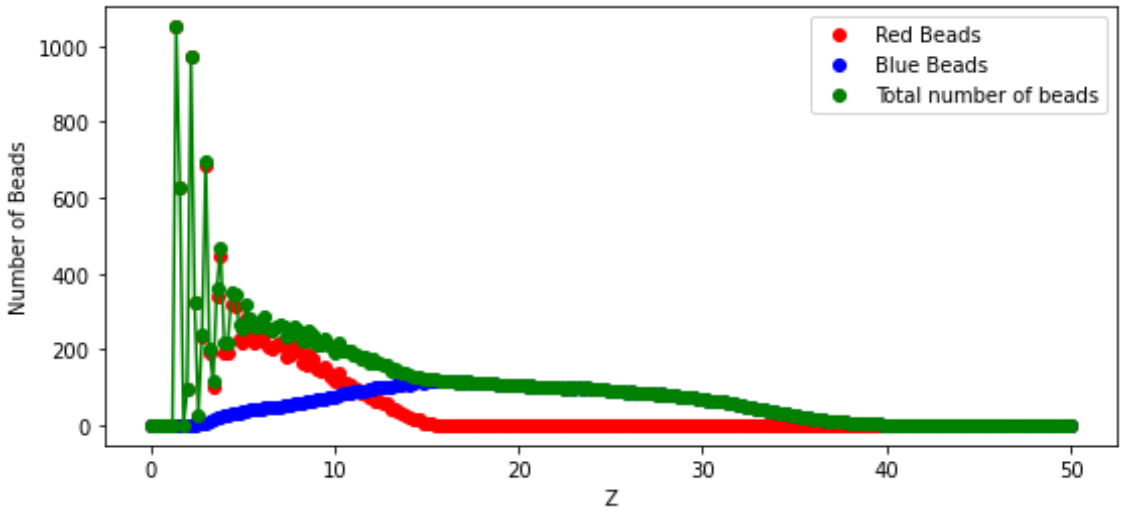

Figure 4.6: Number of beads with respect to their z-distance from the surface for the above system

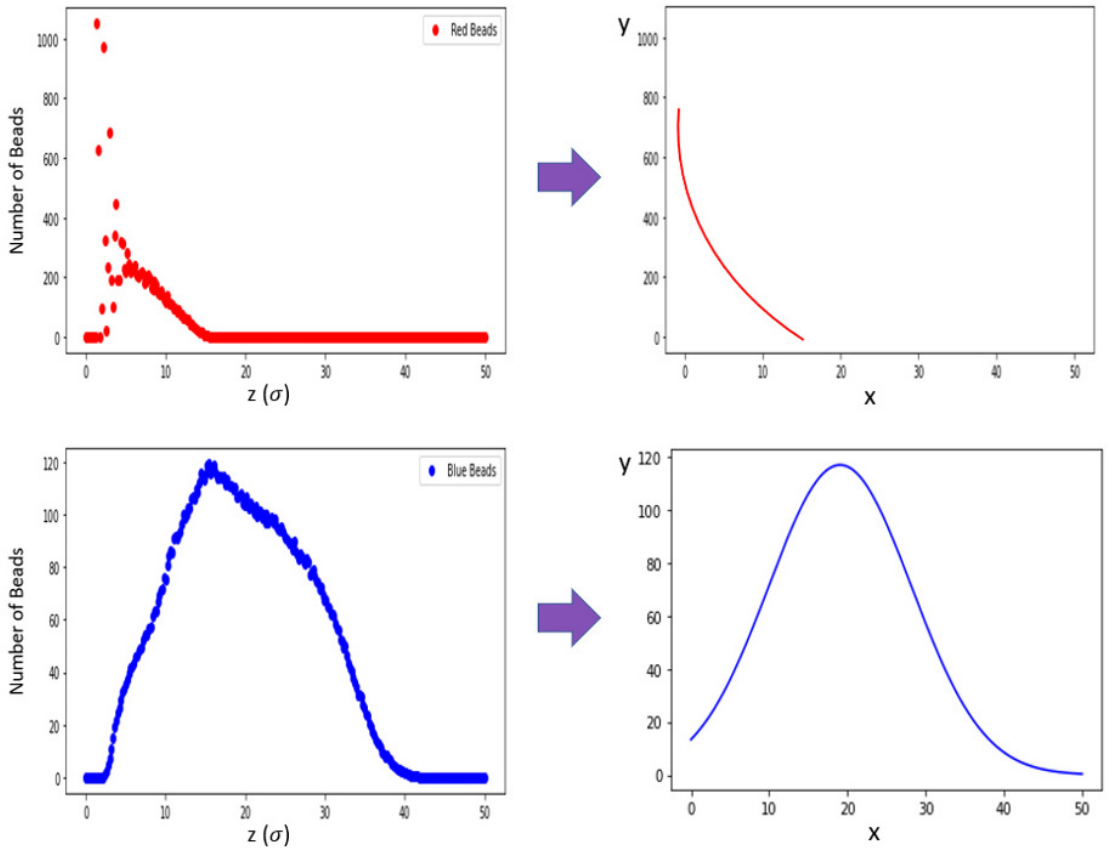

Figure 4.7: plots showing the number of red beads and blue beads above the surface, the curves fitted on the pattern of beads are exponential and gaussian functions for red and blue beads, respectively.

A similar scenario happens when the strength of attractions modified from $u = 5KT$ to $u = 15KT$. In this system, the number of red beads increases on the surface (Figure 4.8, Figure 4.9). The fitting functions are $351.61 \times \exp(-0.09 \times x) - 19.10$, and $118.44 \times \exp(-(x - 18.63)^2/(2 \times 9.031^2))$ for the concentration of red beads and blue beads, respectively.

In all the three systems, the curves corresponding to red beads are exponential and the curves corresponding to blue beads are gaussian functions. However, the values for the parameters in each function is different from others. The variations are more obvious between the strength of interactions with $u = 5KT$ and $u = 10KT$ also between $u = 5KT$ and $u = 15KT$. The differences in parameters can be neglectable for the systems with the strength of interaction $u = 10KT$ and $u = 15KT$.

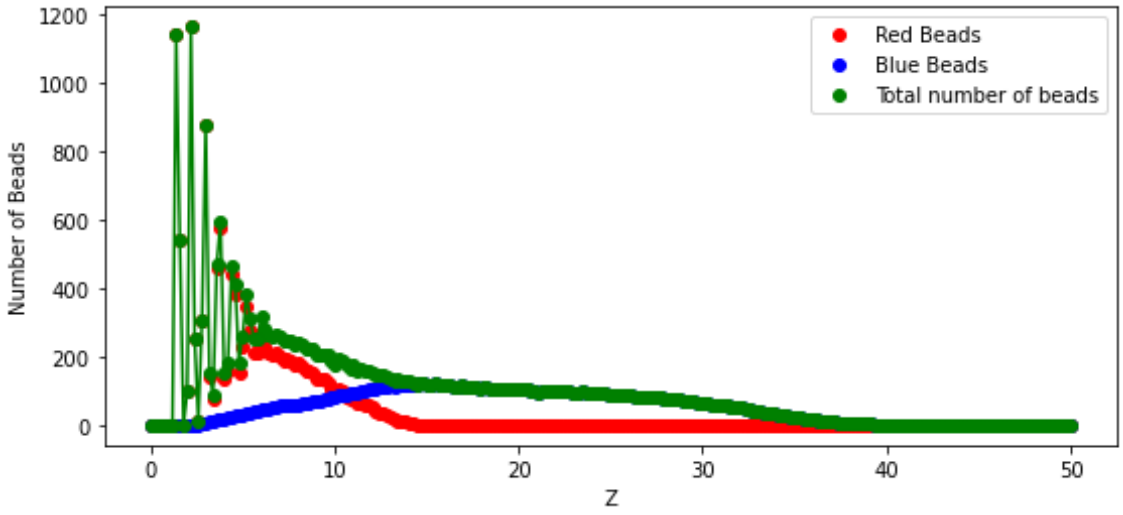

Figure 4.8: Number of beads with respect to their z-distance from the surface when strength of attractions increases to $u = 15KT$

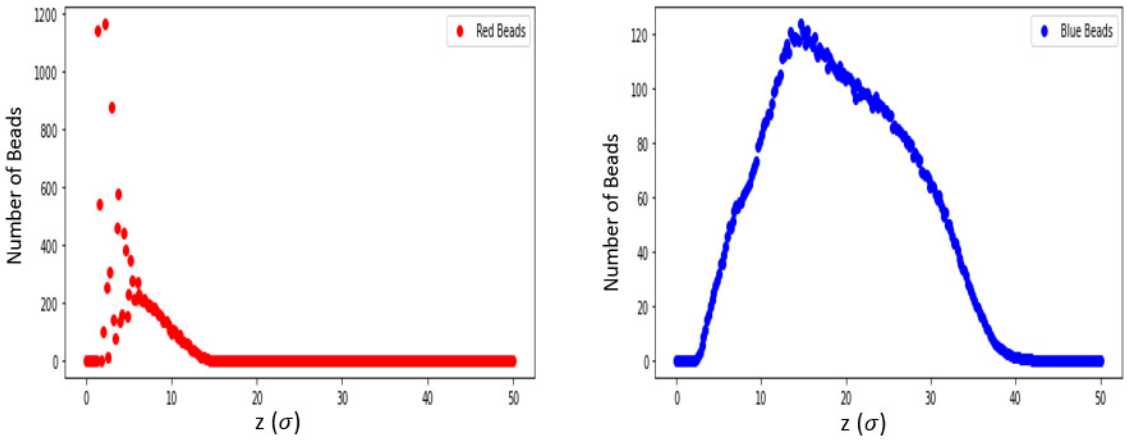

Figure 4.9: plots showing the number of red beads and blue beads above the surface for the system with the strength of attractions increases to $u = 15KT$, the concentration of red beads increases in comparison to the systems with $u = 10KT$ and $u = 5KT$.

We also examined how the strength of attractions between red beads can affect co-polymer adsorption. Accordingly, we changed the attraction from $u = 5KT$, and $u = 10KT$, and $u = 15KT$ to $u = 2KT$. In the system with the attractions of $u = 5KT$ between red beads and the surface and the strength of attraction $u = 2KT$ between red beads, there would be some red beads which do not get near the surface at the end of the simulation. However, they make multitude of clusters and spread above the surface. As it is shown in Figure 4.10, co-polymers are not absorbed to the surface.

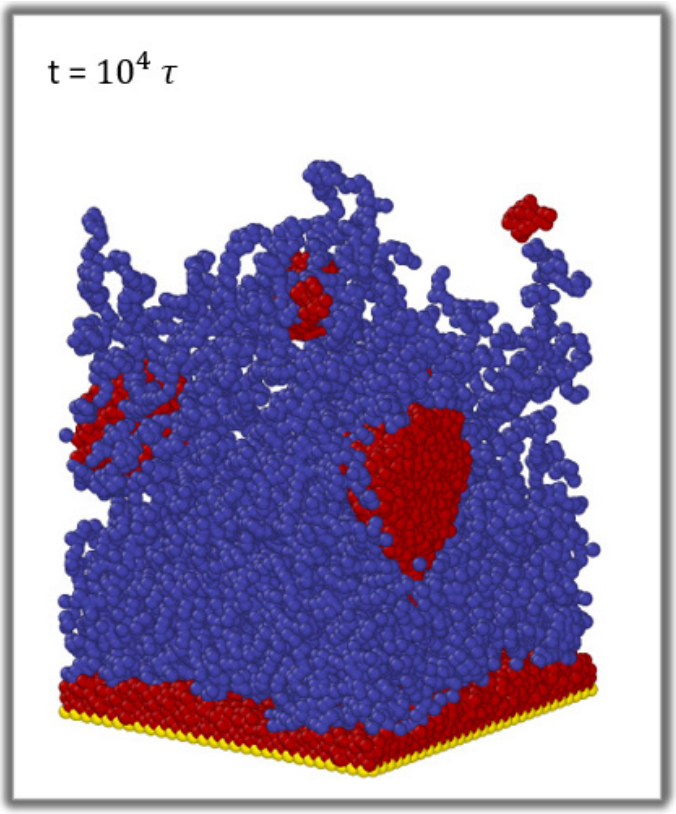

Figure 4.10: Snapshot of simulation, the last frame of the simulation where the strength of attractions between red beads and the surface is $u = 5KT$, and between red beads and themselves is $u = 2KT$, here blue beads repulse each other with the strength of interaction $u = 2KT$.

For the systems with the strength of attractions between red beads and the surface are $u = 10KT$ and $u = 15KT$ where the attraction between red beads is $u = 2KT$, we have all the red part of the co-polymers near the surface, and the blue beads on top of them. In Figure 4.11 and Figure 4.12, the last frame of the according simulations has been shown. Besides, the concentration profile of beads has been plotted in Figure 4.13. As it was expected, the population of red beads close to the surface is more in the system with stronger attractions between the surface and red beads. In both systems, the strength of repulsions as well as the strength of attractions between red beads are the same. However, the only difference is the attractions between the surface beads and the red beads.

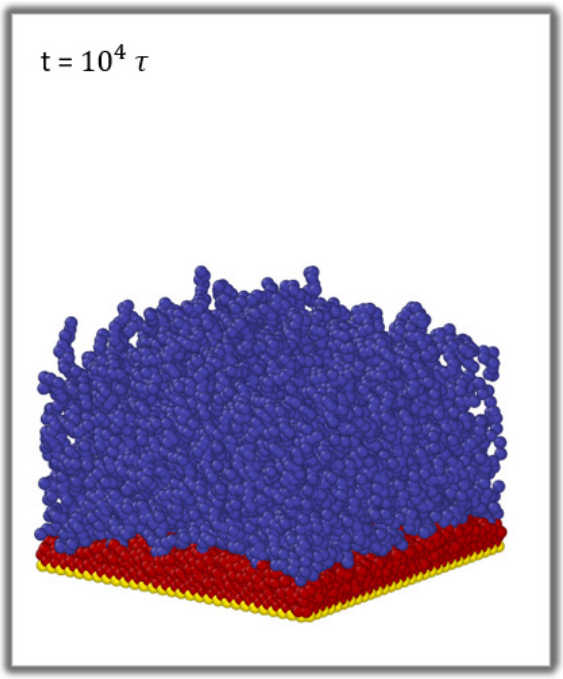

Figure 4.11: Snapshot of simulation, the last frame of the simulation where the strength of attractions between red beads and the surface is $u = 10KT$, and between red beads and themselves is $u = 2KT$

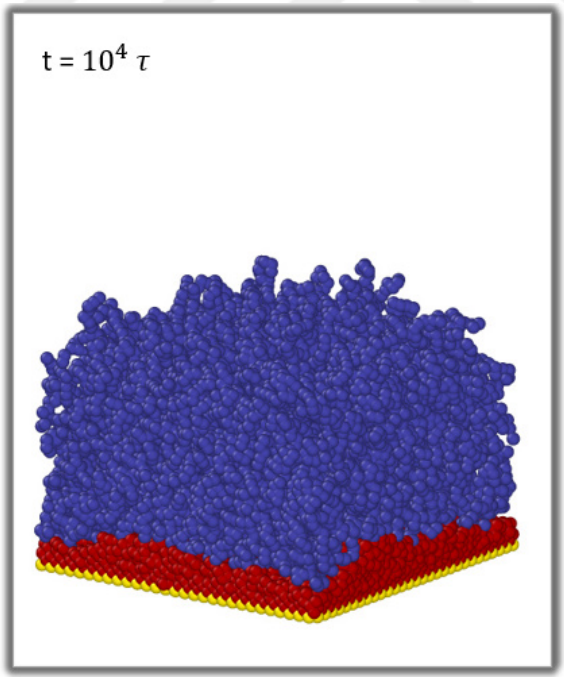

Figure 4.12: Snapshot of simulation, the last frame of the simulation where the strength of attractions between red beads and the surface is $u = 15KT$, and between red beads and themselves is $u = 2KT$

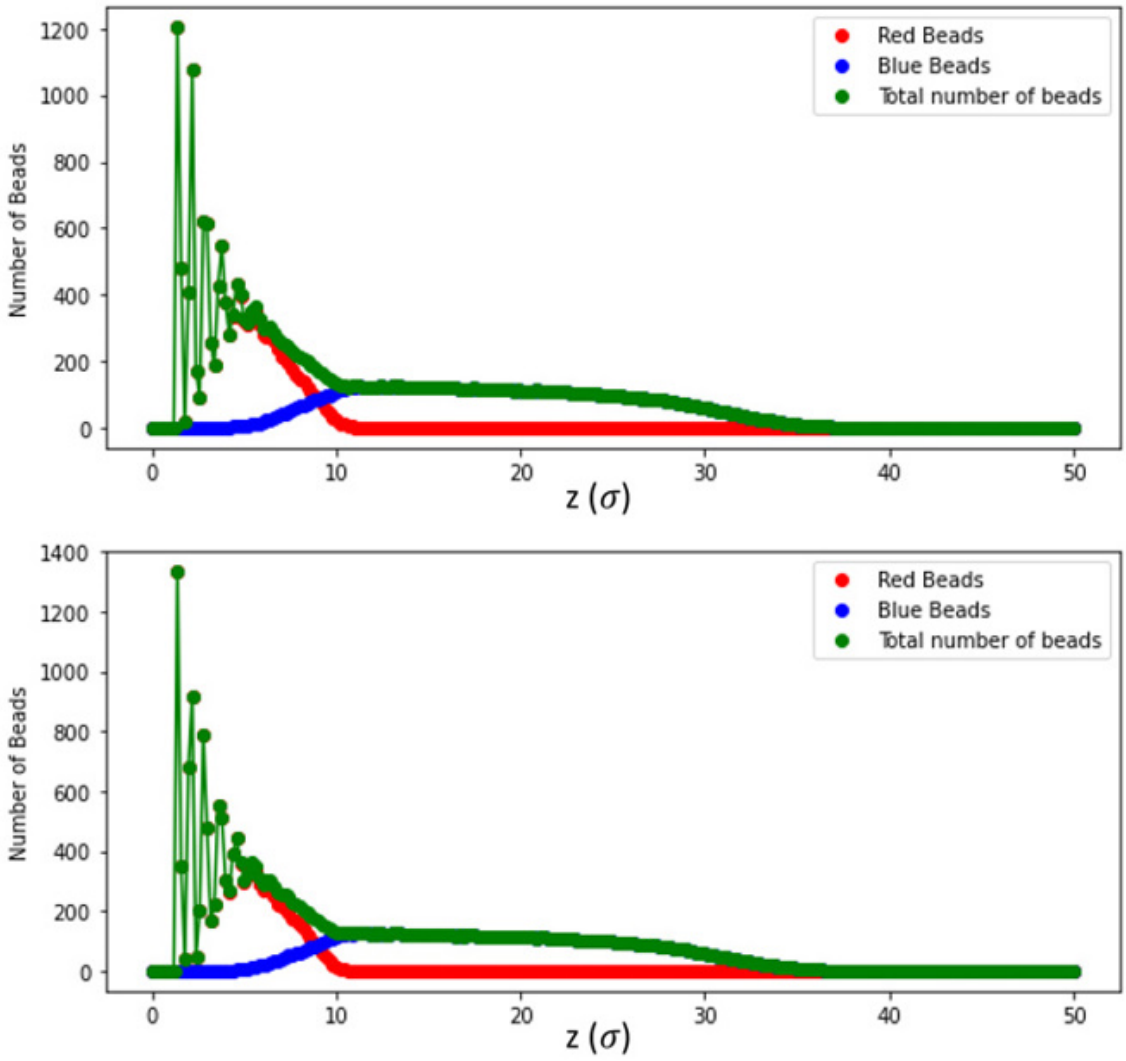

Figure 4.13: Number of beads with respect to their z-distance from the surface, the upper plot is for the system with the strength of attractions $u = 10KT$ between red beads and the surface, the lower plot is for the system with this attraction of $u = 15KT$.

The value of parameters of exponential and gaussian fitting curves (for red beads and blue beads, respectively) for the systems are as follows. For the system with the attractions of $u = 10KT$, we have $394.68 \times \exp(-0.11 \times x) - 18.27$, and $130.95 \times \exp(-(x - 18.30)^2/(2 \times 8.18^2))$. Also, for the case of $u = 15KT$, they are $400.54 \times \exp(-0.11 \times x) - 17.92$, and $131.69 \times \exp(-(x - 18.19)^2/(2 \times 8.14^2))$. The variations of parameters are very small for the two systems.

Compared to the systems where the strength of attractions between red beads are the same as the attractions between the surface and red beads, in these systems (attractions

between red beads decreased to $u = 2KT$) more red beads assemble near the surface.

4.3. The effect of number of co-polymers on adsorption process

To examine how the population of beads of the whole system alter adsorption process, we utilized another system in which the number of co-polymers decrease from 256 to 144. Except for the number of chains, all the features regarding the di-block co-polymers in both systems are the same. Also, we kept the volume fraction (mentioned in chapter 3) approximately identical for the two systems, which is 7%. For this section, we stayed with the same strengths of interactions, which are $u = 5KT$ and $u = 10KT$ for the attractions between red beads and the surface. The strength of repulsions is $u = 2KT$, and attractions between red beads is $u = 5KT$ and $u = 10KT$ for the first and the second systems, respectively.

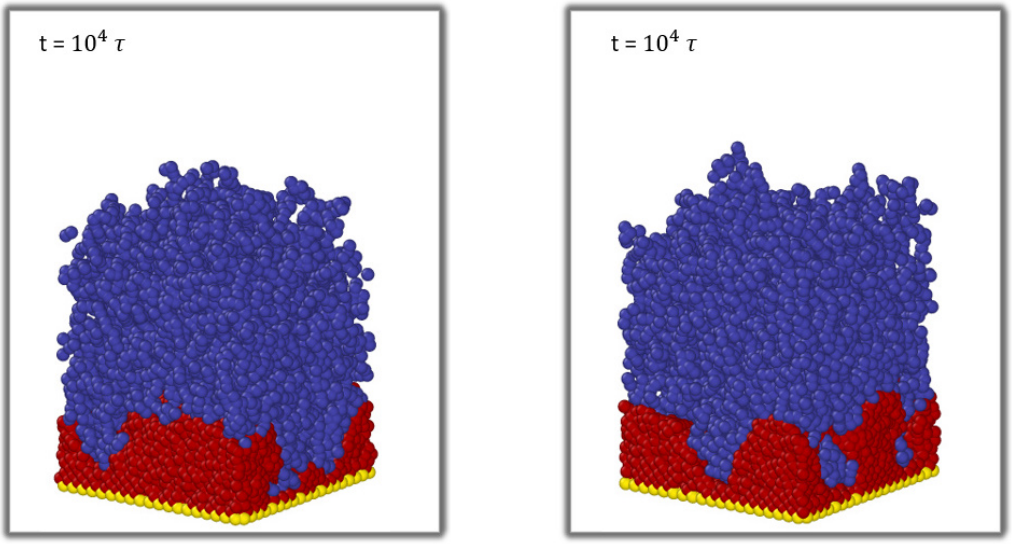

Figure 4.14: Snapshots of two simulations, the image in the left is the last frame of the simulation where the strength of attractions between red beads and the surface is $u = 5KT$, and between red beads and themselves is $u = 5KT$; the image in the right side is the last frame of the simulation with where the strength of attractions between red beads and the surface is $u = 5KT$, and between red beads and themselves is $u = 5KT$. The repulsive interactions are $u = 2KT$.

As it is shown in Figure 4.14, red beads gather on the surface, and blue beads are distributed on top of the region like the systems with 256 co-polymer chains and the same interactions. However, the red mass built on the surface does not have a well-organized shape (like the system with 256 chains in the previous section), and it is like blue beads penetrate the region. We obtained the concentration profile of beads for the systems (Figure 4.15 and Figure 4.16). Both of the red and blue graphs have similar patterns to the previous systems', but there are some deviations in the patterns that makes them different from the previous graphs (as it is shown in Figure 4.15 and 4.16). The curves fit on the graphs are still exponential and gaussian.

The curves are $184.83 \times \exp(-0.08 \times x) - 13.42$ for red beads, and $67.20 \times \exp(-(x - 21.72)^2/(2 \times -8.99^2))$ for blue beads in the system with $u = 5KT$. Besides, for the system with $u = 10KT$, the curves obey the same functions as $188.59 \times \exp(-0.08 \times x) - 12.96$ for red beads, and $68.47 \times \exp(-(x - 21.37)^2/(2 \times -8.84^2))$ for blue beads.

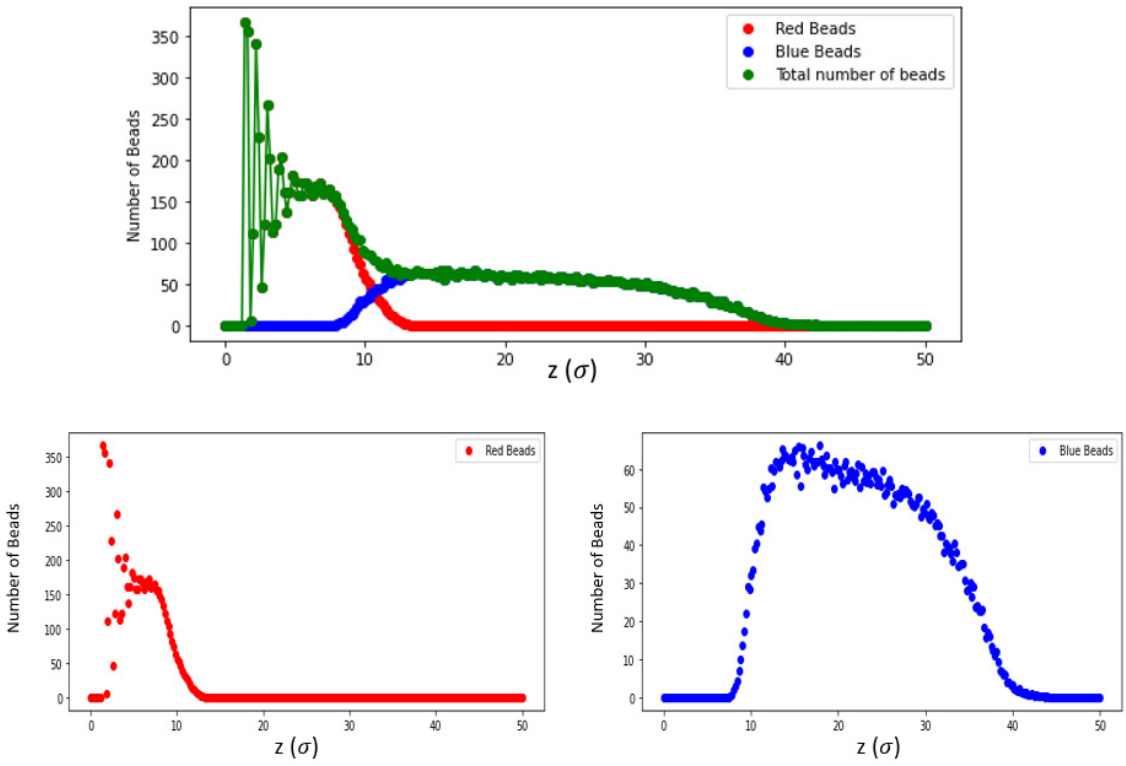

Figure 4.15: plots showing the number of red beads and blue beads above the surface for the 144-copolymer system with the strength of attractions increases to $u = 10KT$

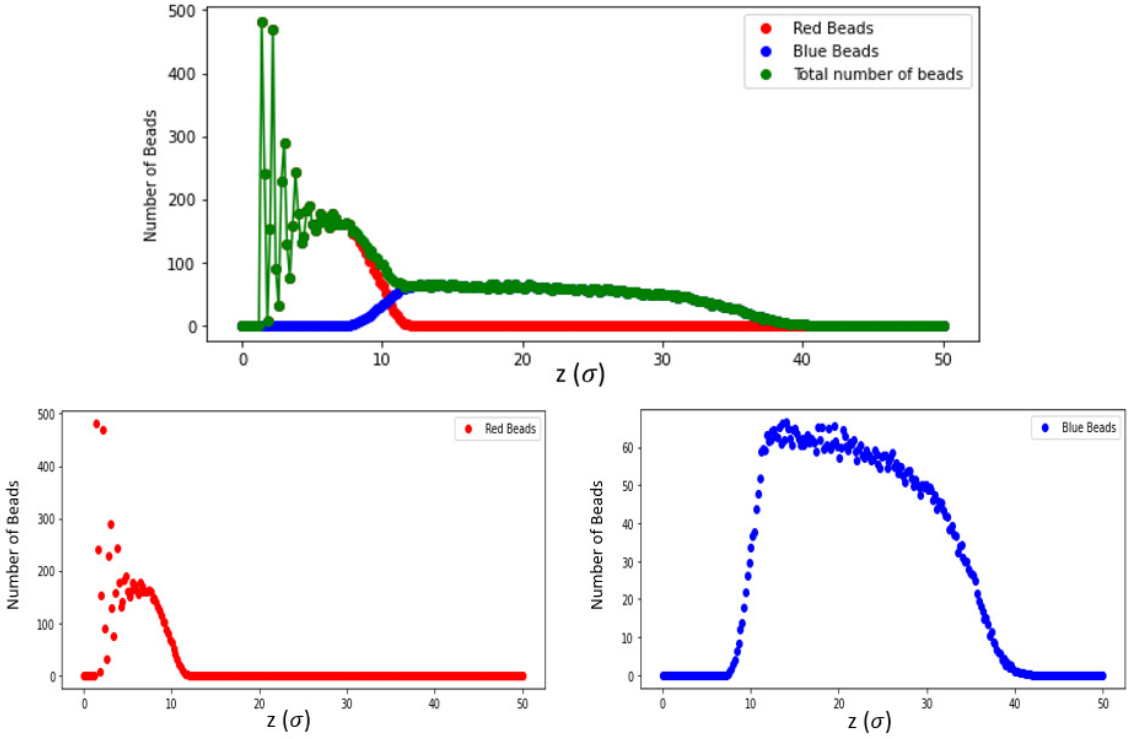

Figure 4.16: plots showing the number of red beads and blue beads above the surface for the 144-copolymer system with the strength of attractions increases to $u = 15KT$

4.4. The effect of proportion of different beads in a co-polymer on adsorption process

To examine how various percentages of red and blue beads along co-polymers can affect the adsorption process, we considered three organization of di-block co-polymers where red beads construct 25%, 50%, and 75% of each chain. The configurations that we studied till now have the co-polymers 50% of whom were consists of red beads (50 beads out of 100 beads). In this section, we added the co-polymers each with 25 red beads and 75 blue beads, and also with 75 red beads and the rest blue beads. The total number of chains remains 256 for all the systems.

As it is shown in Figure 4.17, when the percentage of red beads is 25, then, all the beads do not assemble on the surface. On the other hand, the attractions acting among red beads cause them to make clusters of red beads which are moving above the surface.

Moreover, the height of co-polymers does not decrease like the previous di-block co-polymers (chains with 50% red beads). This does not happen for the system with 75% of the structure of each chain made up of red beads. Here, co-polymers shrink on the surface. Red beads gather on the surface and build a red construction, and blue beads move on top of the area (Figure 4.18). To analyze the process better, the concentration profile of beads was plotted. The pattern of the number of beads is far different for the system with 25% red beads in comparison to the previous system (with 50% red beds) as it is expected (Figure 4.19). The results for the system with 75% blue beads are still different from the previous system, but it has similarities with it (Figure 4.20). Here, red beads are concentrated near the surface; however, their profile does not obey exponential function. Blue beads are also similar to the blue beads' profile in the previous system. From the results, one can claim that as the percentage of red beads (the beads that are attracted by the surface) goes up, the dynamical behavior of the system seems more like the system with di-block co-polymers consists of the same number of red beads and blue beads. When the percentage of red beads decreases, it is more like that some red beads can scape from the surface. Therefore, the would not be adsorbed on the surface.

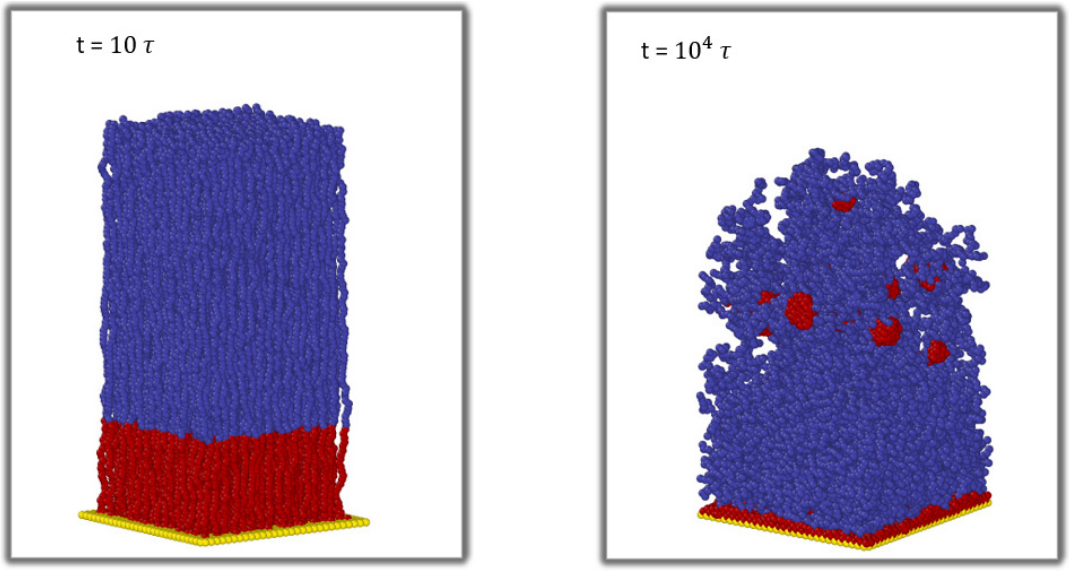

Figure 4.17: Snapshots of a simulation, a frame of relaxation time (left image), and the last frame of the simulation (right image) where 25% of each co=polymer consists of red beads; the image in the right side is the last frame of the simulation where 75% of each co=polymer consists of red beads. The strength of attractions is $u = 5KT$, and the strength of repulsive interactions is $u = 2KT$.

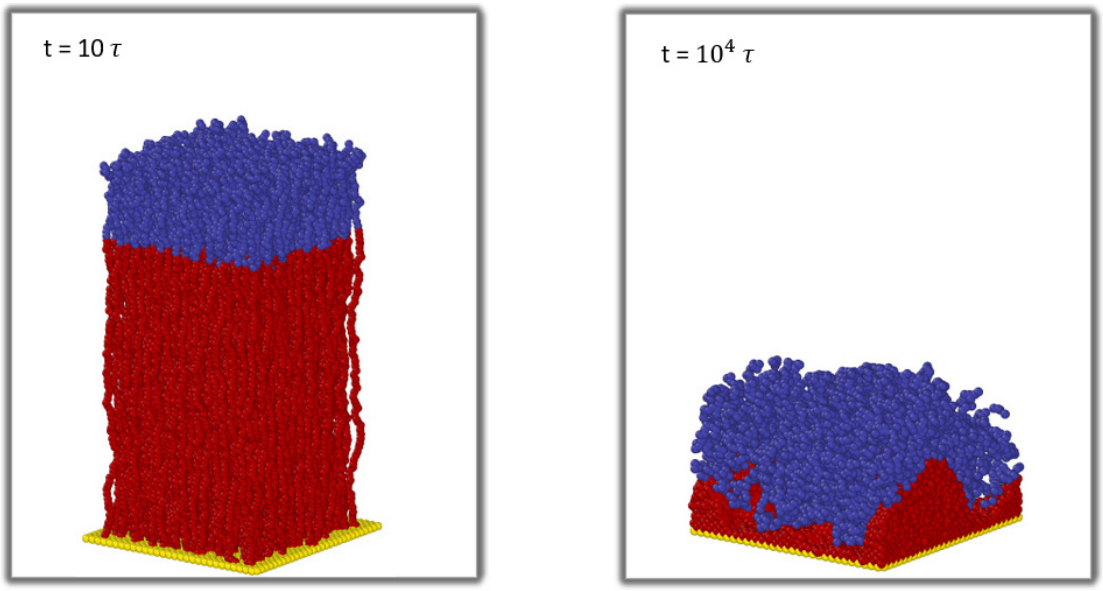

Figure 4.18: Snapshots of a simulation, a frame of relaxation time (left image), and the last frame of the simulation (right image) where 75% of each co=polymer consists of red beads. The strength of attractions is $u = 5KT$, and the strength of repulsive interactions is $u = 2KT$.

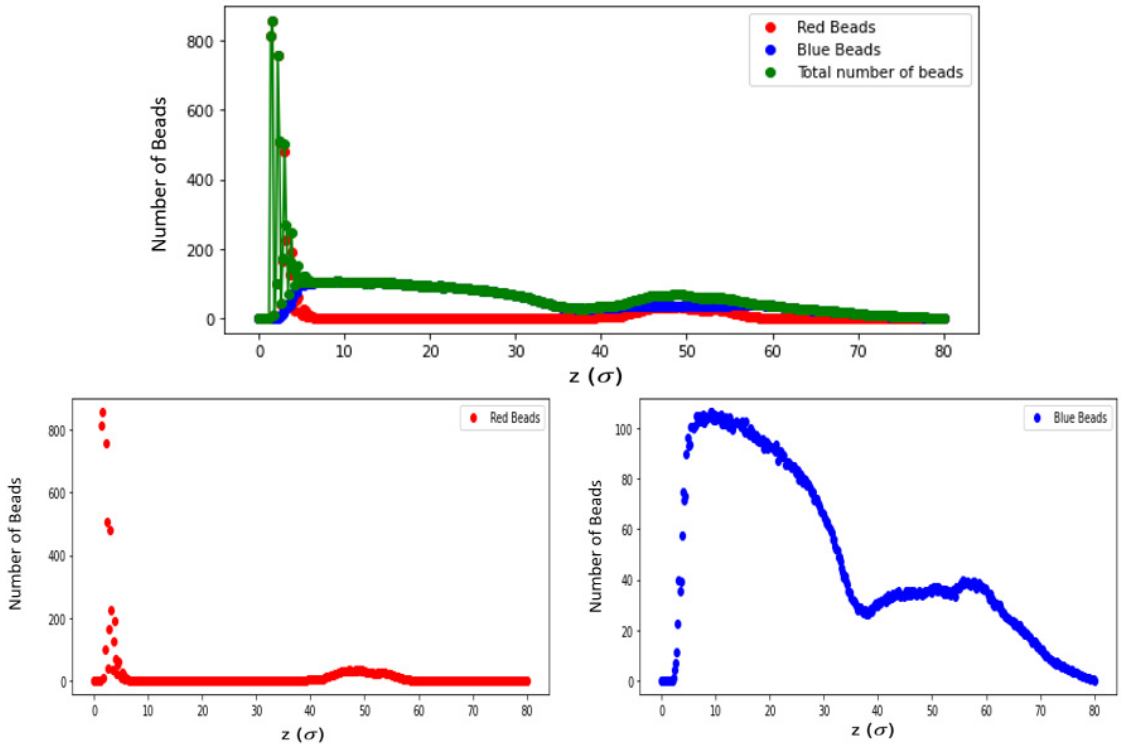

Figure 4.19: plots showing the number of red beads and blue beads above the surface, the according system possesses co-polymer chains that 25% of each are made of red beads.

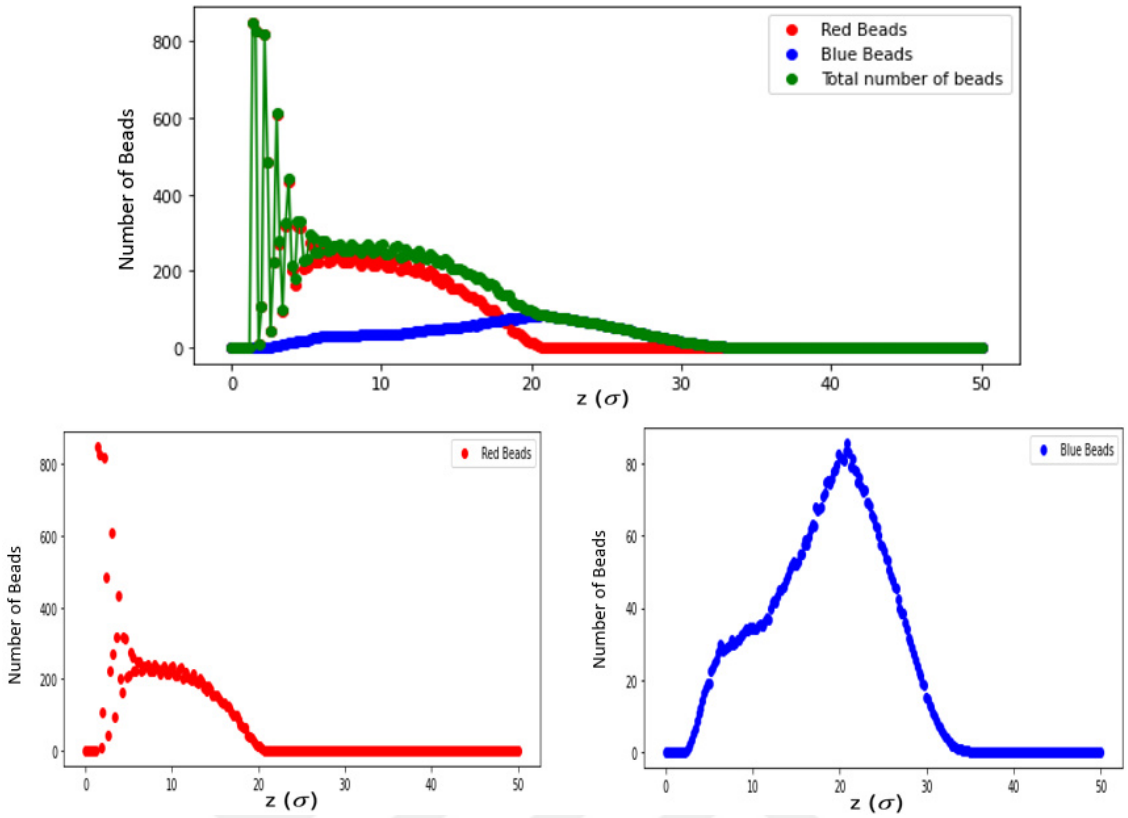

Figure 4.20: plots showing the number of red beads and blue beads above the surface, the according system possesses co-polymer chains that 75% of each are made of red beads. The strength of attractions is $u = 5KT$ in the system.

Furthermore, we replicated the two above systems with the stronger interactions, which are the strength of attractions $u = 10KT$. Unlike the previous system where interactions were weaker, for this case, the co-polymers that 25% of their beads are in red get assemble on the surface. In addition, for both the red and blue concentration profile, we could fit approximate curves which are exponential and gaussian functions. In the configuration, where 75% each co-polymer consists of red beads, we still have all the red beads on the surface like the previous system. As it is shown in Figure 4.21, the only contrast between this system and the previous one with weaker attractions is that the topology of the red mass built on the surface is different from the previous case (in Figure 4.18, image in the left side). As a result, the concentration profile for red and blue beads appears different (Figure 4.23). The pattern of blue beads obeys a gaussian function.

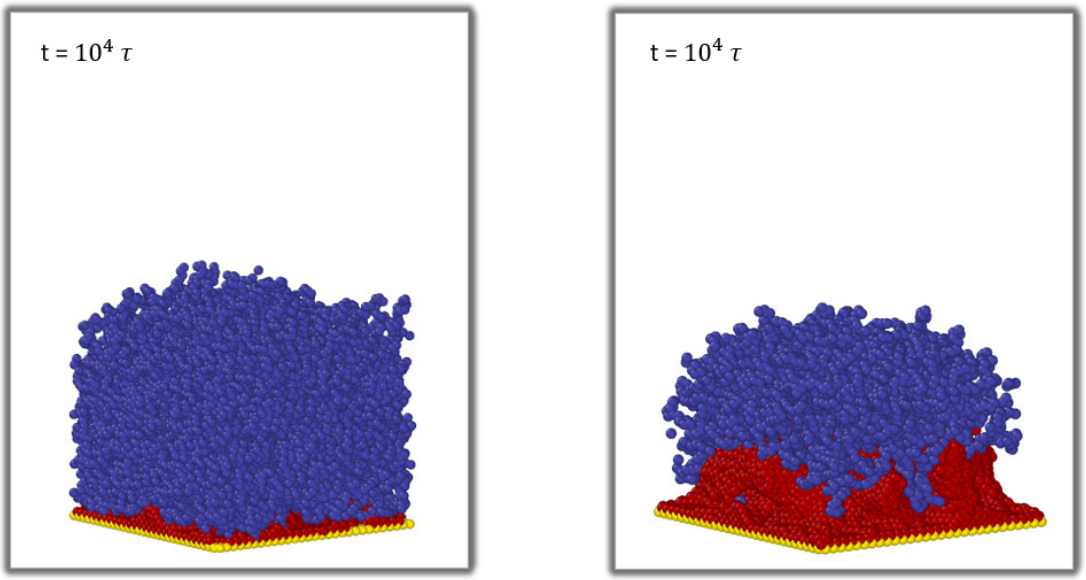

Figure 4.21: Snapshots of two simulations, the image in the left is the last frame of the simulation where 25% of each chain is red; the image in the right side is the last frame of the simulation with where 75% of every chain consists of red beads. The strength of attractions is $u = 10KT$, and the repulsive interaction is $u = 2KT$ for both of them.

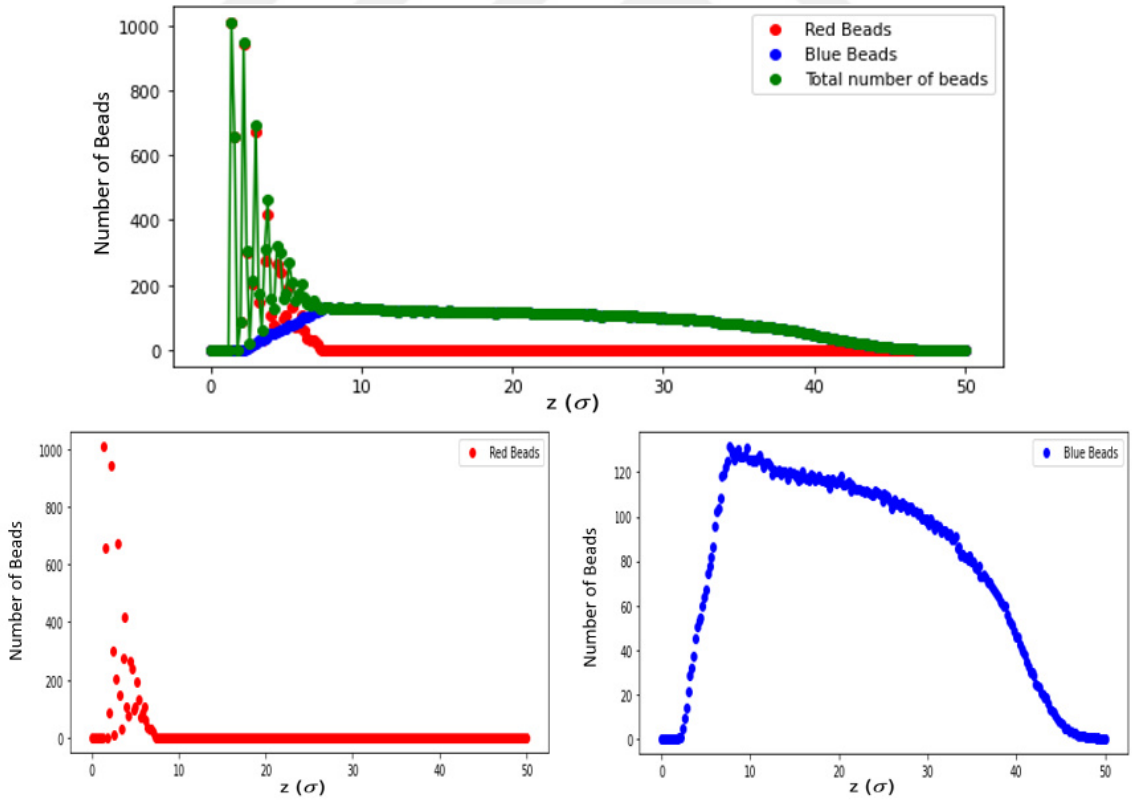

Figure 4.22: plots showing the number of red beads and blue beads above the surface, the according system possesses co-polymer chains that 25% of each are made of red beads. The strength of attractions is $u = 10KT$ in the system.

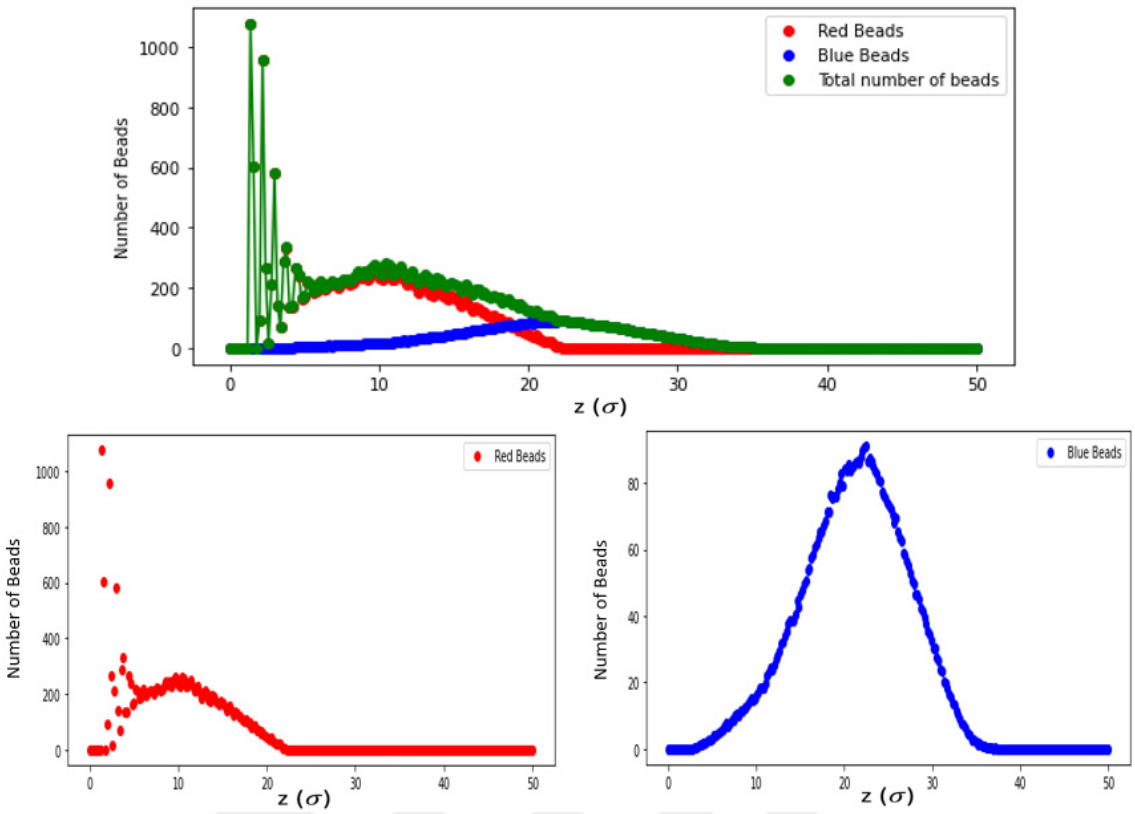

Figure 4.23: plots showing the number of red beads and blue beads above the surface, the according system possesses co-polymer chains that 75% of each are made of red beads. The strength of attractions is $u = 10KT$ in the system.

4.5. Co-polymer brush

As already described, polymer brushes are special structures of polymer chains which are tethered to another object like a surface or another chain. In this section, we wanted to measure the height of co-polymer brushes created above the surface. As it is expected, the red part of co-polymers assembles near the surface making a red layer on it, and the blue beads are located on top of this layer jiggling around. In this way, they can make brushes of the co-polymers above the surface. Investigating the changes in the brushes can shed more light on the aspects of surface-adsorption process.

We, first, quantified the height of brush in the system with the co-polymers (a half of each copolymer have 50 red beads, and the other are blue beads) that are attracted by the surface with $u = 5KT$ (the first configuration in result section). As the number

of frames obtained from the simulations exceeds 400 frames, we ignore some of them which are in the first 20% of the simulations. As it is shown in Figure 4.24, the height of co-polymer brush, which is defined as the blue part of the chains shaking around, starts from 25σ when the system is relaxed. Then, it begins to decrease till it reaches to a steady state which is 15σ.

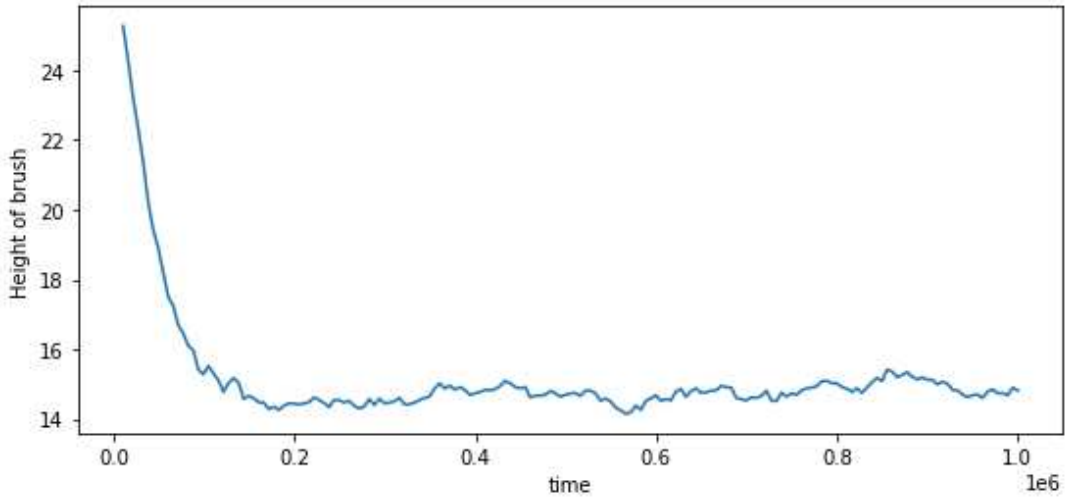

Figure 4.24: graph representing the changes in the co-polymer brush through the process, in this system, the number of chains is 256, the proportion of red and blue beads in each co-polymer chain is one, and the strength of attractions is $u = 5KT$, and the strength of repulsions is $u = 2KT$.

In addition, we compared the height of brushes in three systems with different strengths of attractions. To do so, we picked up the last 20% of the simulation frames. As it is shown in Figure 4.25, the average height of the brush decreases when the strength of interactions goes up.

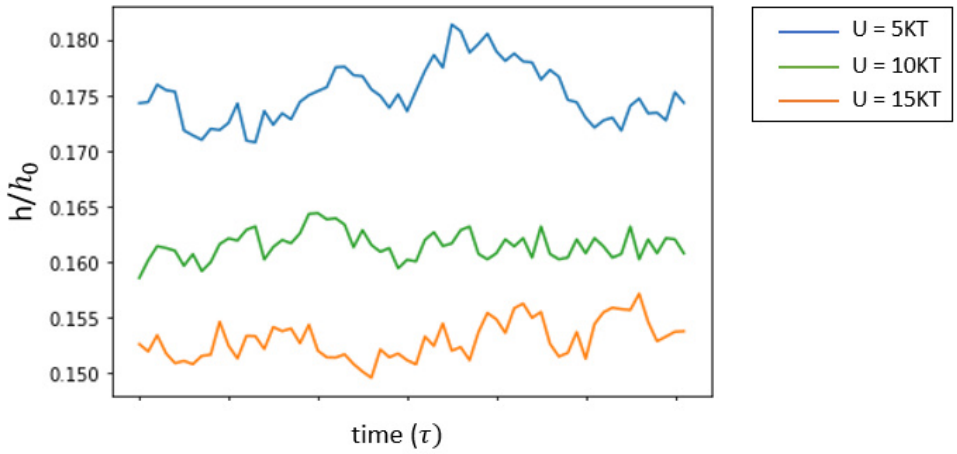

Figure 4.25: plot representing the changes in the co-polymer brush for three systems through the process; for all of them, the number of chains is 256, and the proportion of red and blue beads in each co-polymer chain is one; the strength of attractions varies from $u = 5KT$ to $u = 15KT$.

4.6. Loop formation

When polymers attach to a surface, they can form loops on the surface. In this section, we quantified the number of loops and the lengths of them. Firstly, we consider the systems with 256 co-polymers. Figure 4.24 shows the frequency of loops when the strength of attractions between the surface and red beads is $u = 5KT$.

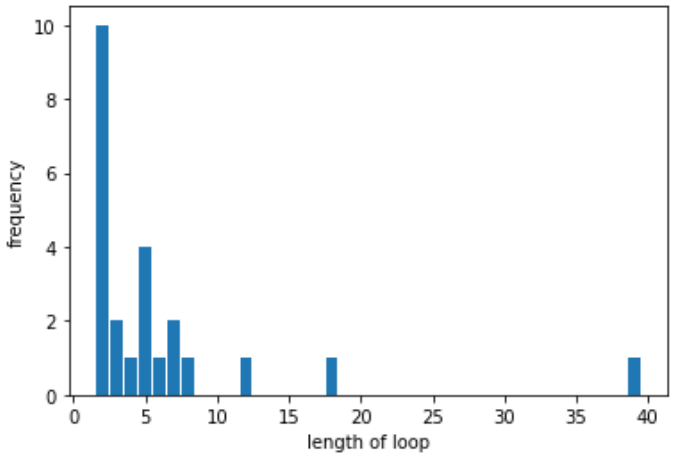

Figure 4.26: chart representing the total number of loops created on the surface is 24. The smallest loop has the length of 2 meaning that it consists of 4 beads (two of them are attached to the surface), and it has the most frequency among other lengths of loops. The largest loop has the length of 39 beads.

Figure 4.25 and Figure 4.26 show how frequency of loops changes with the length of loops for the systems where strength of attractions is $u = 10KT$ and $u = 15KT$, respectively. According to the figures below, it can be concluded that by increasing the strength of attractions the maximum size of loop drops. This means the chance of floating above the surface decreases for beads when they are attracted by the surface intensively. The attractions between the surface and the beads overcomes the attractions between red beads.

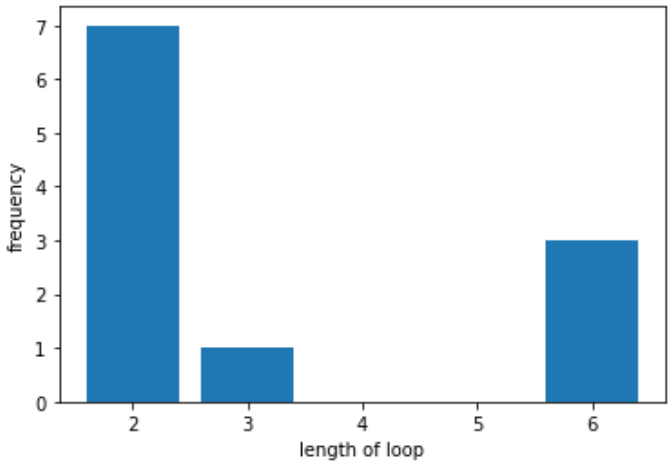

Figure 4.27: chart representing the number of loops created on the surface according to their length, the total number is 11 loops; the maximum length of loops is 6, and the loops with the minimum length of 2 has the most frequency in the system. In this system the strength of attractions is $10KT$.

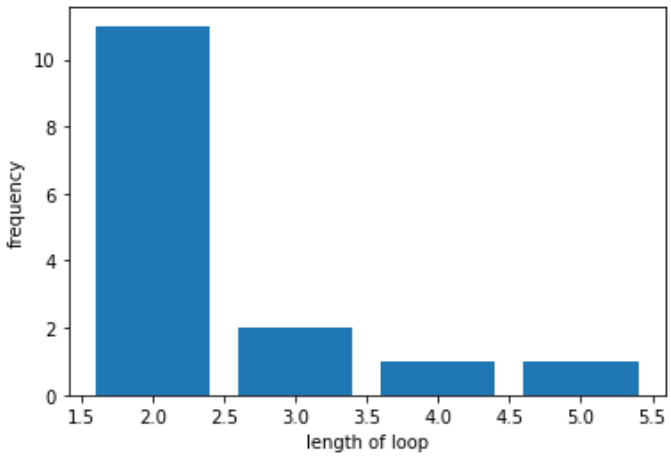

Figure 4.28: chart representing the number of loops created on the surface according to their length; the total number of loops is 15; the maximum size of loops is 5, and the loops with the minimum length of 2 has the most frequency in the system. In this system the strength of attractions is $15KT$.

4.7. The effect of chemical correlation on adsorption process

As already mentioned, the order of monomers along a co-polymer chain can affects the properties of the co-polymer. In chapter 3, we introduced a parameter, which is chemical correlation of chain, to add other co-polymers to our systems. The chemical correlation varies between -1 and 1, which goes back to random co-polymer, tri-block co-polymer, and homo-polymer, respectively. In this section, we examined the effect of the chemical correlations on the adsorption process.

4.7.1 Triblock co-polymers

We designed 256 triblock co-polymers on a surface where the interactions between red beads and the surface beads are of attractions (with the strength of $u = 5KT$). The two blocks constructing chains are of red beads, and the middle block is made of blue beads. Given some time to the initial configuration of the system, triblock co-polymers start relaxing on the surface. During the relaxation of co-polymers, the only attraction is between red beads and the surface, and all the other interactions defined between every component of the system are repulsions with the strength of $u = 2KT$. After relaxing the chains, another attraction part is added to the system which is among red beads with the strength of interaction $u = 5KT$. As it is shown in Figure 4.29, beads get closer to the surface. A layer of red beads is built on the surface, and some other red clusters can be seen above the surface. Also, blue beads are located on top of the layer and among the clusters.

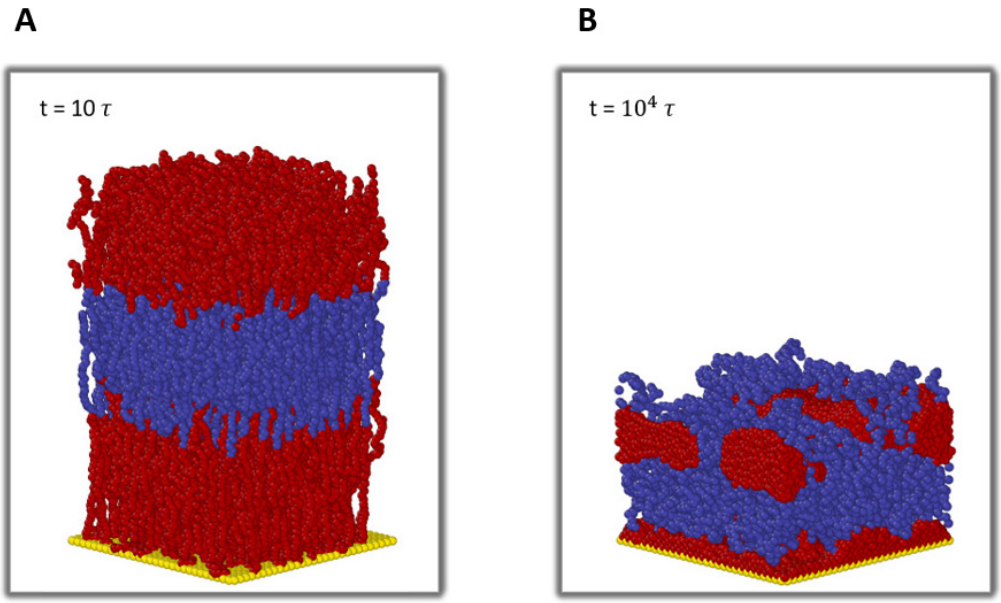

Figure 4.29: Snapshots of the simulation of tri-block co-polymers on the surface; A) a frame of the simulation after the relaxation time, B) the last frame of the simulation

The plots representing the number of beads according to their distance from the surface, shows that two masses of red beads are located near the surface and above it. The red beads in between are the clusters shown in Figure 4.29. The pattern of distribution is not comparable with di-block co-polymers (the previous system). Blue beads still keep the whole pattern of distribution as the ones in previous system. However, it does not accord with any gaussian function, and has two peaks on the graph.

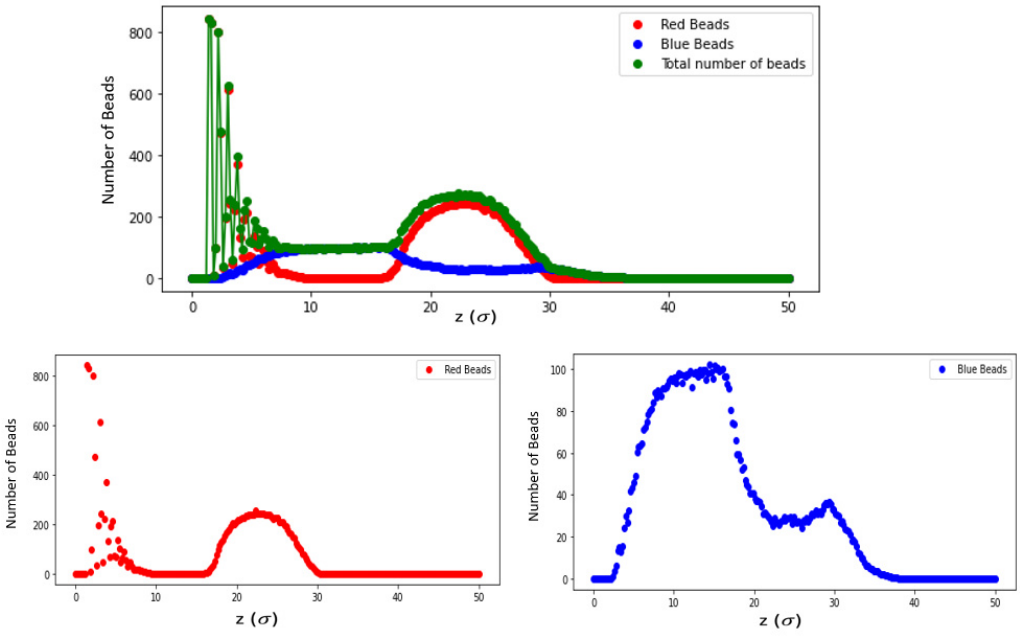

Figure 4.30: plots showing the number of red beads and blue beads above the surface

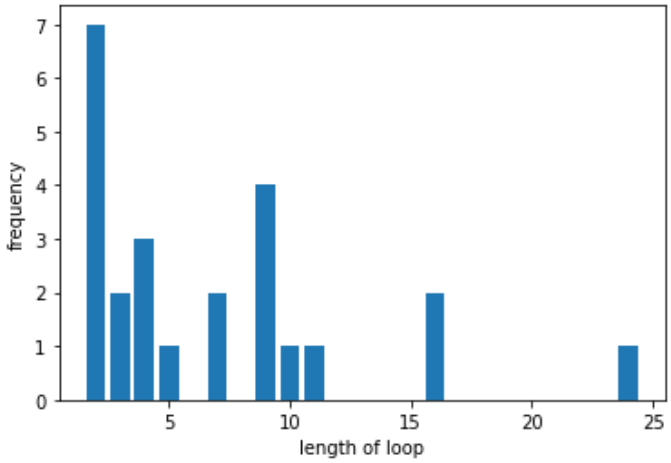

Figure 4.31: chart representing the number of loops created on the surface according to their length, the total number is 24 loops; the maximum length of loops is 24, and the loops with the minimum length of 2 has the most frequency in the system. In this system the strength of attractions is $5KT$.

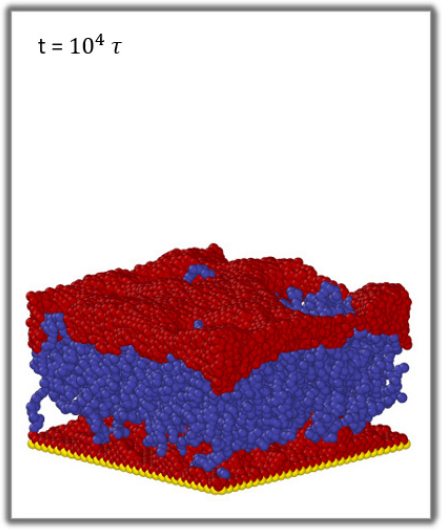

Figure 4.32: Snapshot of the simulation of tri-block co-polymers on the surface; the last frame of the simulation of tri-block co-polymers on the surface, and the strength of attractions increased to $u = 10KT$.

In Figure 4.32 (the above image) shows a snapshot from tri-block co-polymers attracted on the surface with a different strength of attraction with is $u = 10KT$ (It is twice the attractions in Figure 4.29). According to Figure 4.33, the concentration profile of red beads in this system is quite similar to the previous system (in Figure 4.30), but the pattern regarding the blue beads is symmetric and has visible differences with the

previous system.

Moreover, like di-block co-polymers, the maximum size of loops formed on the surface in triblock co-polymers reduces by increasing the strength of attractions between red beads and the surface. However, the total number of loops drops in the according system. Based on Figure 4.31 and Figure 4.34, by modifying the attractions from $5KT$ to $10KT$, the largest loop size changes from 24 beads to 16 beads. Also, the total number of loops reduces from 24 to 6 loops.

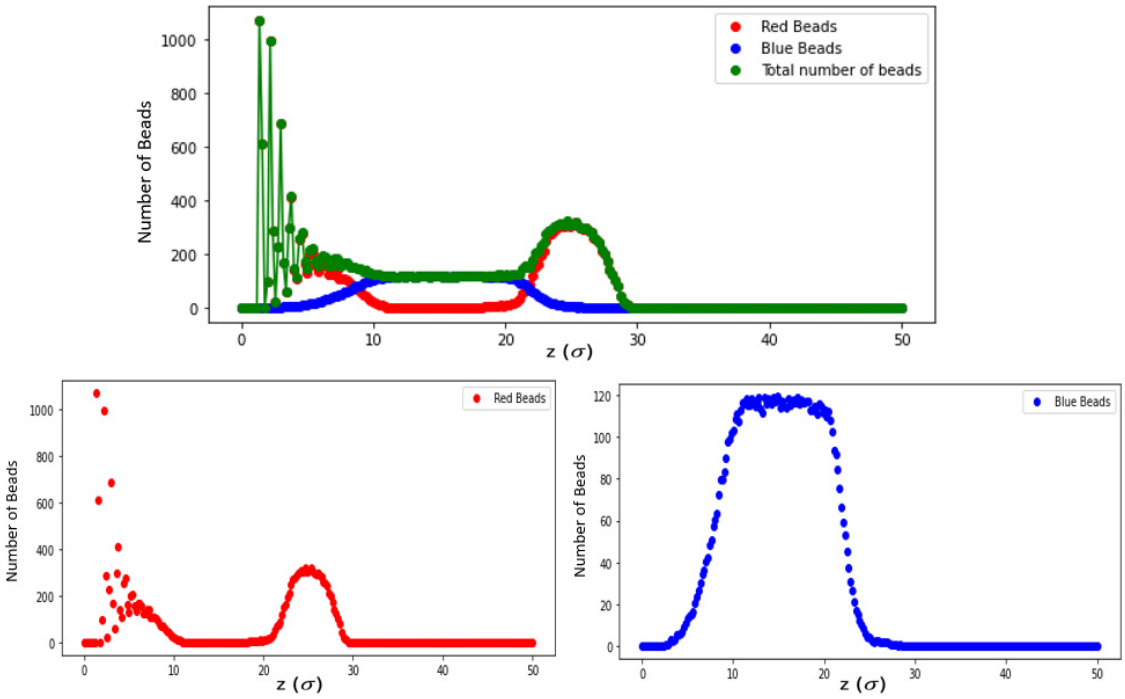

Figure 4.33: plots showing the number of red beads and blue beads above the surface; $u = 10KT$

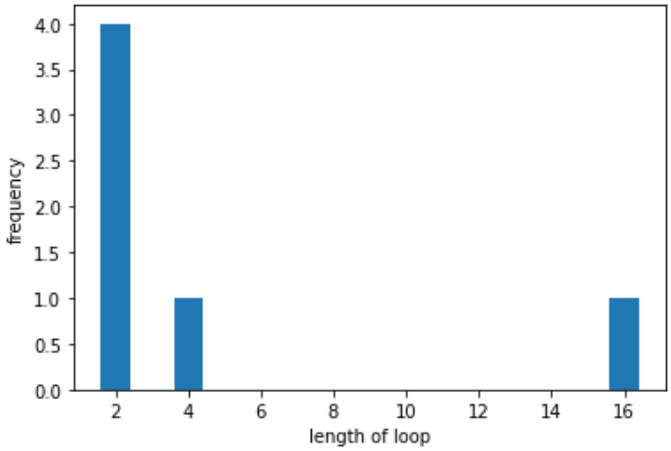

Figure 4.34: chart representing the number of loops created on the surface according to their length, the total number is 6 loops; the maximum length of loops is 16, and the loops with the minimum length of 2 has the most frequency in the system. In this system the strength of attractions is $10KT$.

4.7.2 Random co-polymers

For making random co-polymers, we considered a random pattern produced by random seeds and used it for all the chains in the system. A significant difference between this system and the di-block co-polymers is that, after the chains get relaxed, they go up and increase their distance from the surface (as Figure 4.35 B.). For preventing the chains escaping from the surface, we shrank the simulation box which keeps the chains in appropriate distance from the surface. Therefore, they have the chance to adsorb on the surface.

The concentration profile of the beads appears different from di-block co-polymers. The key feature of them is that the pattern of beads' number above the surface for red beads is very similar to the blue beads.

For this system, we could not recognize any loop on the surface. This makes sense because one of the conditions that we considered for the loop formation is that the beads forming the loop are red beads. As the existence of consecutive red beads in random co-polymers is not common, the chance of finding the successive red beads meeting a

loop's condition is not as much as the di-block or tri-block co-polymers. In this way, we eliminated the condition in which all the beads of loops are necessarily red beads. As a result, we found a relatively larger loops, and the number of loops increases significantly. According to Figure 4.37, the total number of beads counted on the surface is 580.

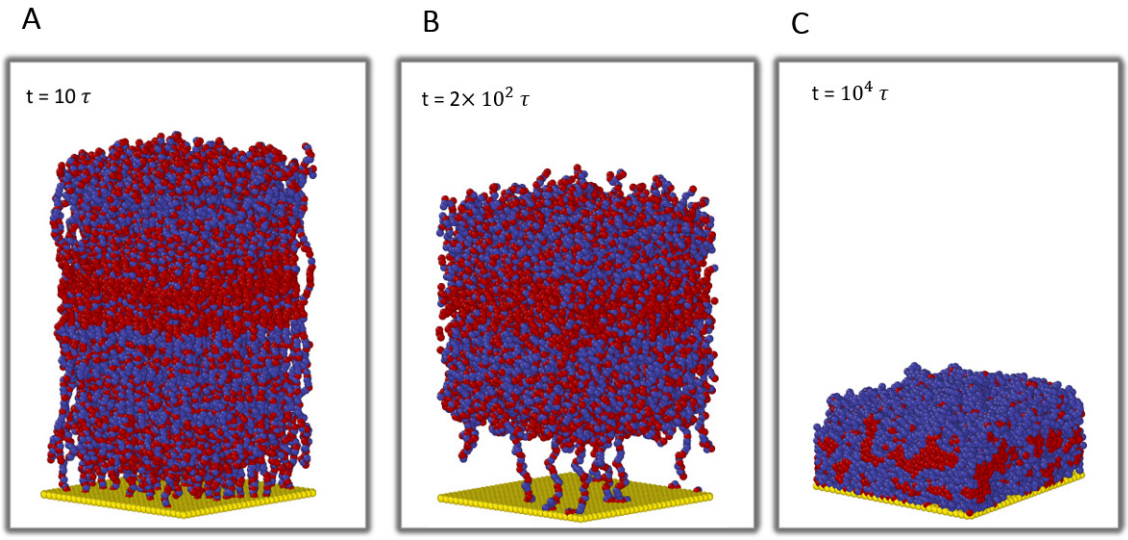

Figure 4.35: Snapshots of the simulation of tri-block co-polymers on the surface; A) a frame of the simulation during the relaxation time, B) a frame of the simulation after the system is relaxed, C) the last frame of the simulation

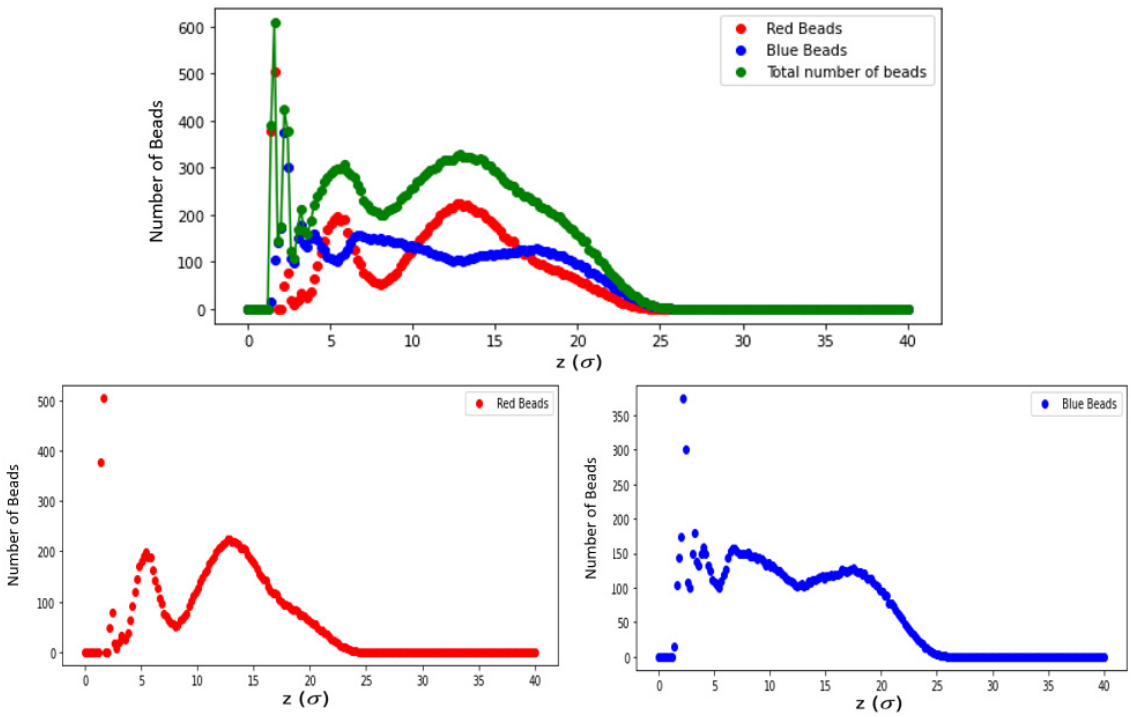

Figure 4.36: plots showing the number of red beads and blue beads above the surface; $u = 5KT$

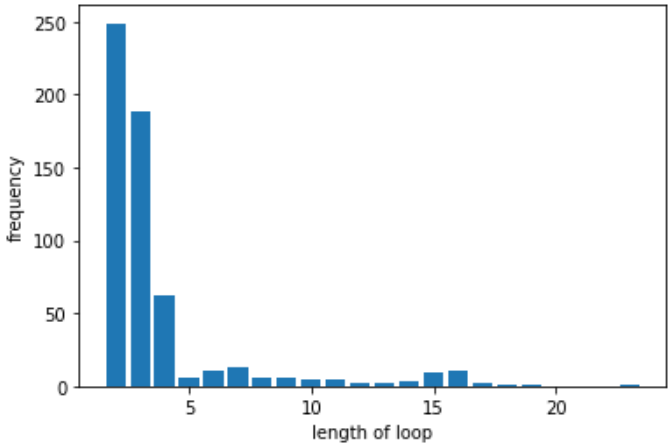

Figure 4.37: chart representing the number of loops created on the surface according to their length, the total number is 580 loops; the maximum length of loops is 23, and the loops with the minimum length of 2 has the most frequency in the system. In this system the strength of attractions is $5KT$.

We replicated the simulation for an increased strength of interaction (10KT). Again, we observed similar patterns of bead concentration for red beads and blue beads. Also, there are peaks in the plots which accords with the previous random co-polymer system with the strength of attractions $u = 5KT$.

In comparison to the system with strength of attraction $u = 5KT$, the total number of loops formed on the surface and also the size of the loops decreases in the current system. According to Figure 4.40, the maximum size of loops is 6 beads, and the number of loops reduces from 580 (for the above system) to 158. The most frequent size of loop is still 3 beads for this configuration.

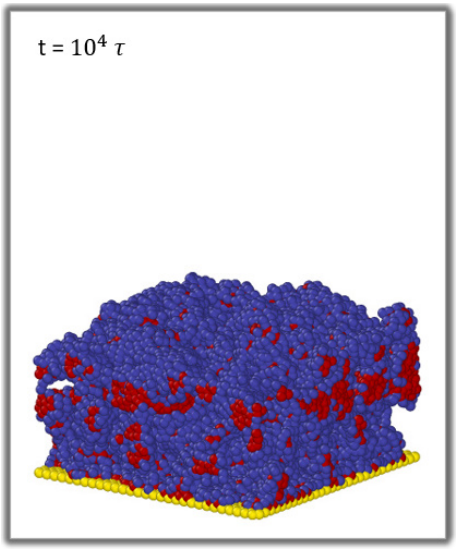

Figure 4.38: Snapshot of the simulation of random co-polymers on the surface; the last frame of the simulation of random co-polymers on the surface, and the strength of attractions increased to $u = 10KT$.

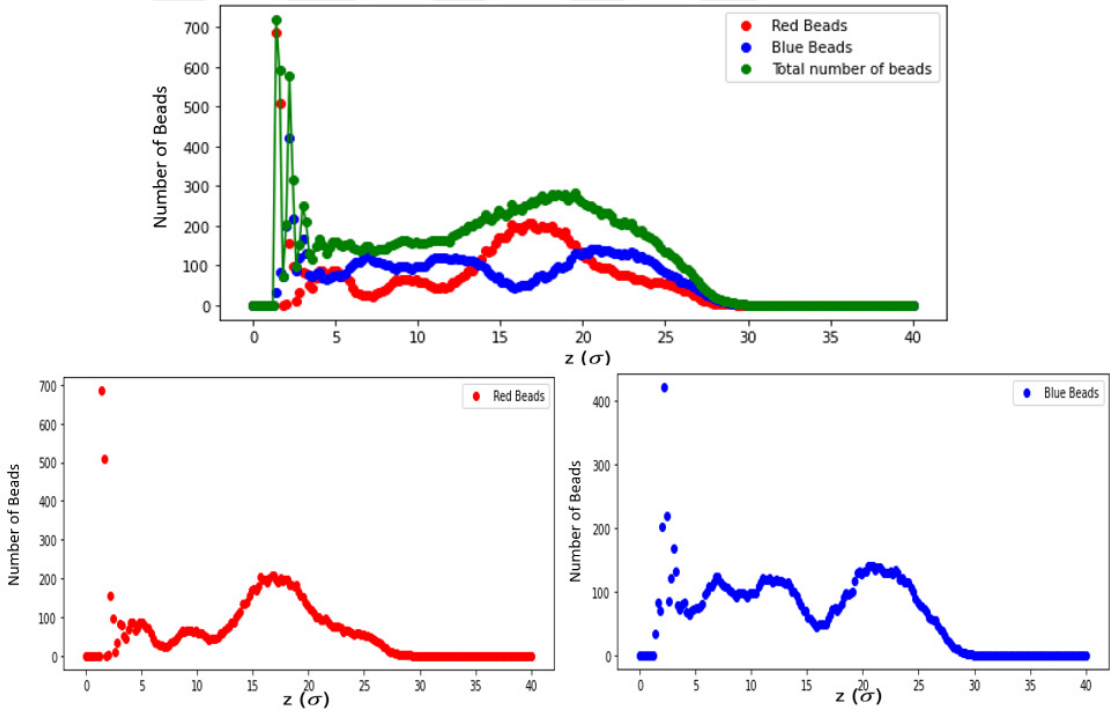

Figure 4.39: plots showing the number of red beads and blue beads above the surface; $u = 10KT$

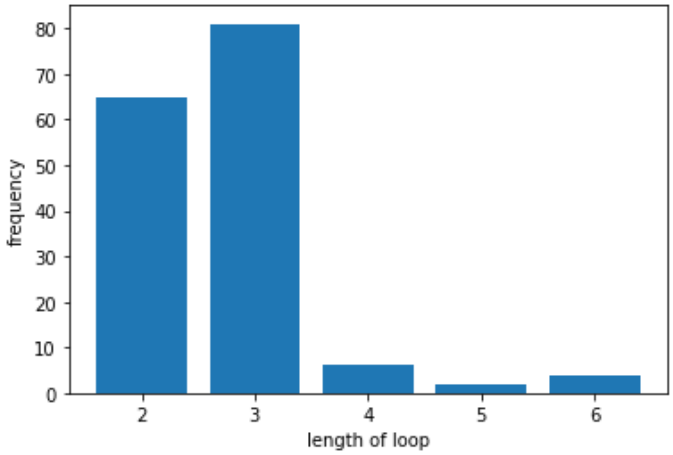

Figure 4.40: chart representing the number of loops created on the surface according to their length, the total number is 158 loops; the maximum length of loops is 6, and the loops with the minimum length of 3 has the most frequency in the system. The strength of attractions is $10KT$.

4.7.3 Homopolymers

We were also interested in surface-adsorption of homopolymers which are built up of only one type of bead. Here, we chose red beads to construct the chains since we were seeking the states where beads can attract to the surface.

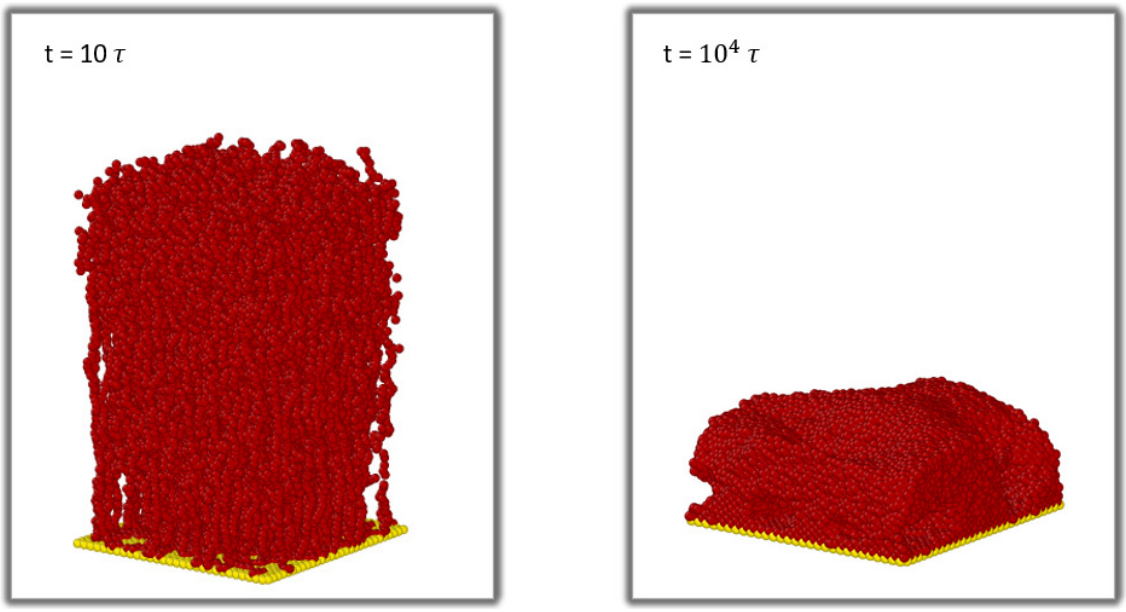

Figure 4.41: 35 Snapshots of the simulation of homopolymers on the surface; A) a frame of the simulation during the relaxation time, B) the last frame of the simulation

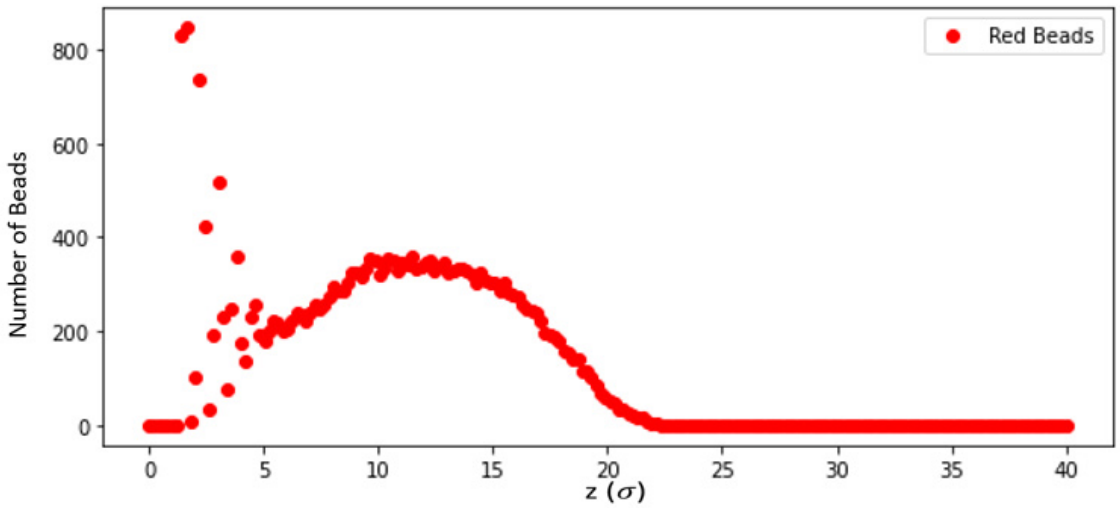

Figure 4.42: plot showing the number of red beads above the surface; the concentration profile fluctuates in lower distances from the surface, then, the pattern looks a gaussian behavior in higher distances. The strength of attractions is $u = 5KT$.

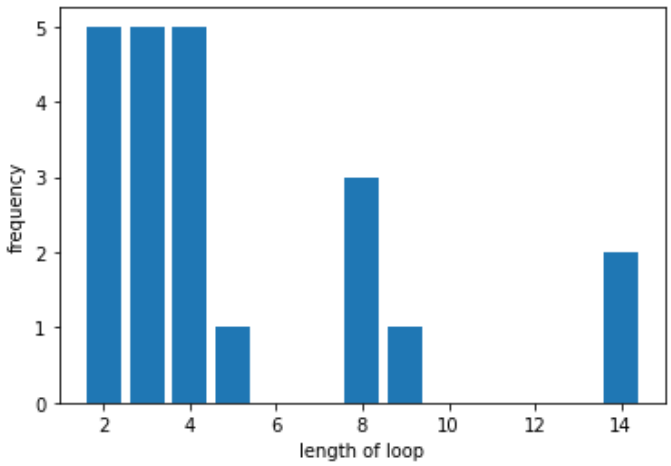

Figure 4.43: chart representing the number of loops created on the surface according to their length, the total number is 18 loops; the maximum length of loops is 14, and the loops with the minimum length of 2,3, and 4 has the most frequency in the system. The strength of attractions is $5KT$.

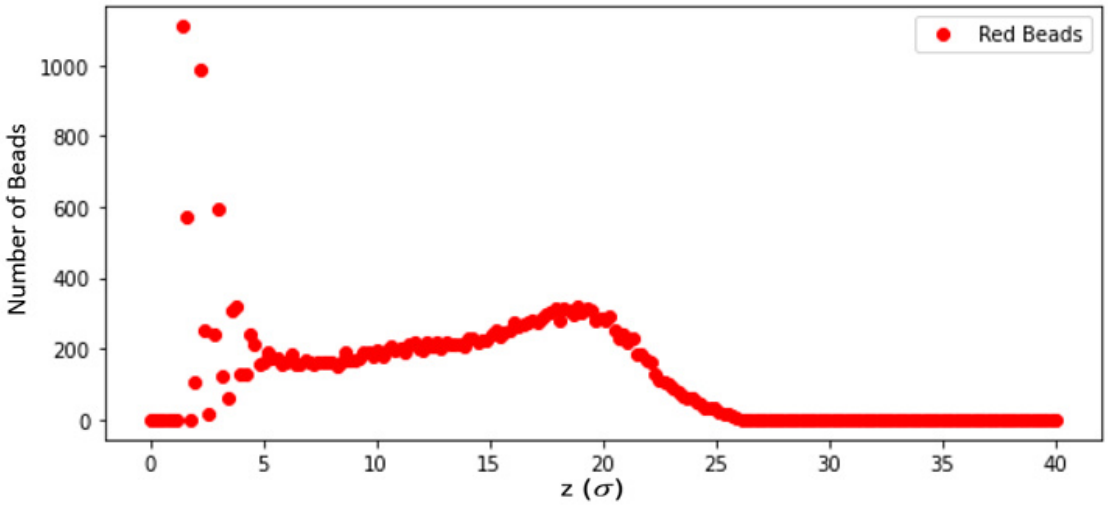

Figure 4.44: plot showing the number of red beads above the surface; the concentration profile fluctuates in lower distances from the surface, then, the patten reaches to a steady state and there is a peak in higher distances. The strength of attractions is $u = 10KT$.

When the strength of interactions increases from $5KT$ to $10KT$, the concentration profile loses its symmetric pattern (if the initial fluctuations get ignored for both of the systems). Besides, as it is expected, the number of beads gather near the surface increases by the growth of strength of interactions (Figure 4.44).

Moreover, there is a significant reduction in the number of loops in the homo-polymer system. This can be explained in this way that as all the beads are attracted on the surface, the conditions in which some beads escape from the surface and the neighboring beads decreases in comparison to other systems (where there are co-polymers). When the strength of interactions increases from $5KT$ to $10KT$, there is also reduction in the number of loops formed on the surface (4.44).

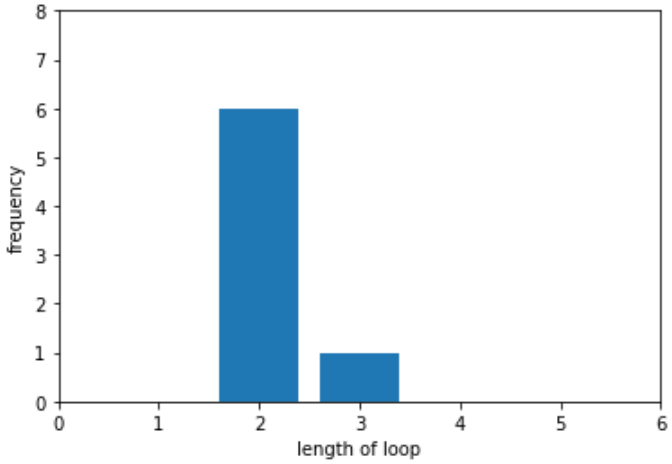

Figure 4.45: chart representing the number of loops created on the surface according to their length, the total number is 7 loops; the maximum length of loops is 3, and the loops with the minimum length of 2 has the most frequency in the system. The strength of attractions is $10KT$.

4.8. The effect of co-polymers arrangement on adsorption process

As a final attempt, we wanted to examine what the process would be if co-polymers are arranged differently on the surface in initial configuration. To do so, we replaced vertical co-polymer chains with horizontal co-polymers which are distributed randomly on the surface. We tried it for various co-polymers with identical chemical correlations.

The first contrast between the previously vertical chains and the new system with horizontal chains is the extent of strength of interactions which work for each of the two systems to make the co-polymers attracted on the surface. Unlike the previous system, the strength of attractions smaller than $u = 5KT$ is enough to get the chains near the surface. Therefore, we restricted the attractions to $1KT$, $2KT$, $3KT$, $4KT$, and $5KT$.

The second difference is that there are totable number of clusters made of red beads moving above the surface in the new system. Although the height of co-polymer chains seems to decrease and the area of the surface is covered by a layer of red beads and on top of them a layer of blue beads, red clusters jiggling around are observed above the surface.

We began with di-block co-polymers (each chain is made up of 50 red beads and 50 blue beads) and compared the adsorption process for different strengths of interaction. Compared to the system with vertical chains, concentration profiles of the new system do not obey the mathematical functions fit on the previous system. Unlike the previous system where most of red beads are attracted on the surface, here we can see some red beads are not assemble on the surface. On the other hand, they increase the distance from the surface and raise the number of red beads in higher distances in the plot (Figure 4.46). Moreover, as it is shown in Figure 4.46, the concentration of blue beads above the surface does not make a symmetric pattern (as it is in the previous system). Figure 4.47 shows the comparison between different strength of interactions for the same configurations of di-block copolymers. Accordingly, when the strength of attractions increases, in the pattern of blue beads concentration, the first peak on the curve goes down and the second peak goes up. The whole pattern of the bead concentration stays the same.

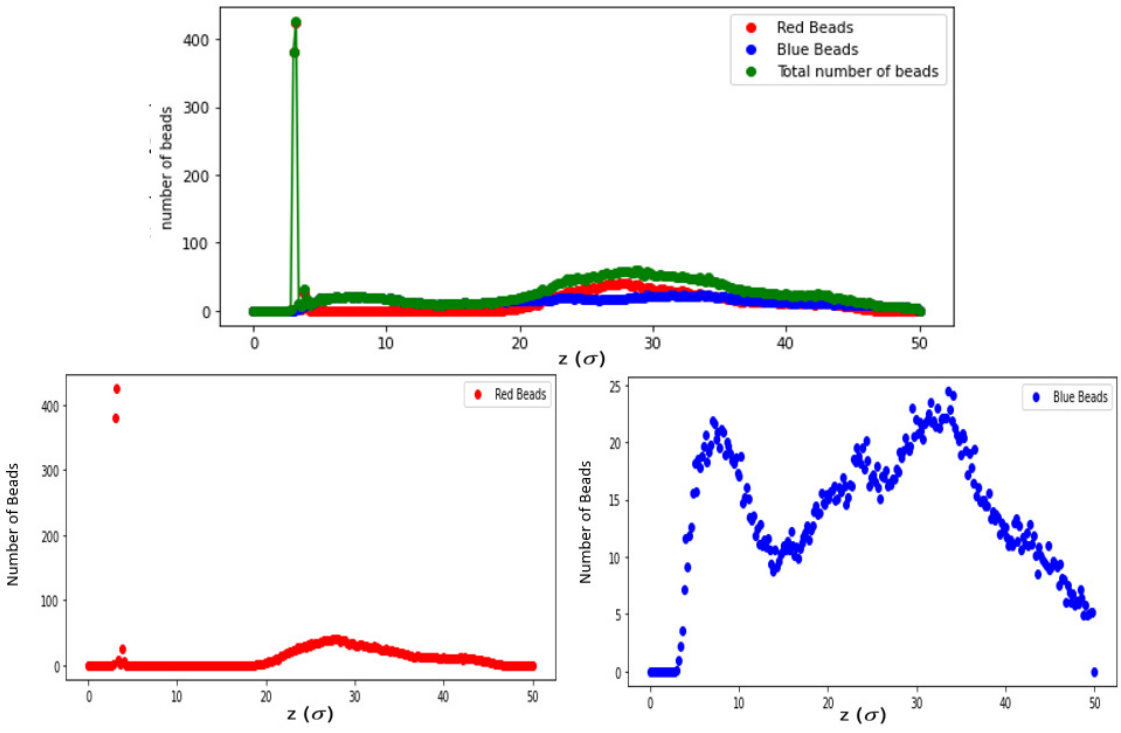

Figure 4.46: plots showing the number of red beads and blue beads above the surface for the system consists of di-block copolymers; $u = 5KT$

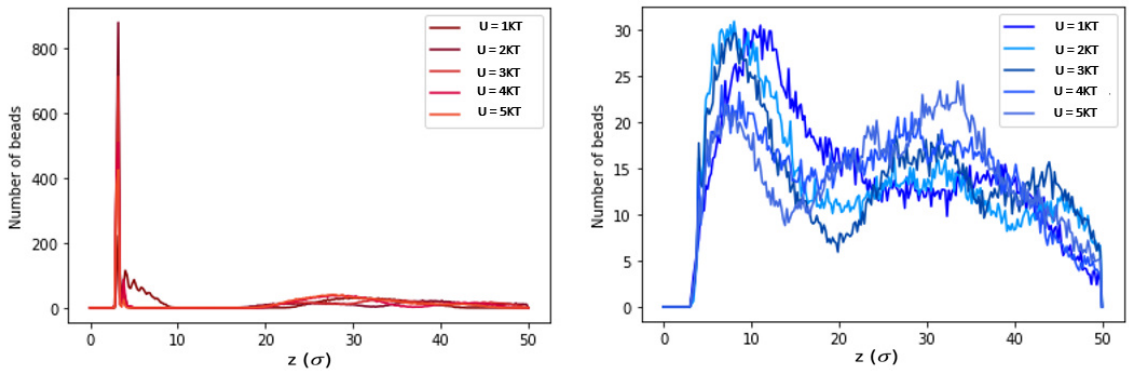

Figure 4.47: plots showing the number of red beads (left) and blue beads (right) above the surface for different strength of interactions

Then, we did the simulations for the systems with tri-block co-polymers, random co-polymers, alternating co-polymers, and homopolymers. The results are shown in Figure 4.48 to Figure 4.51

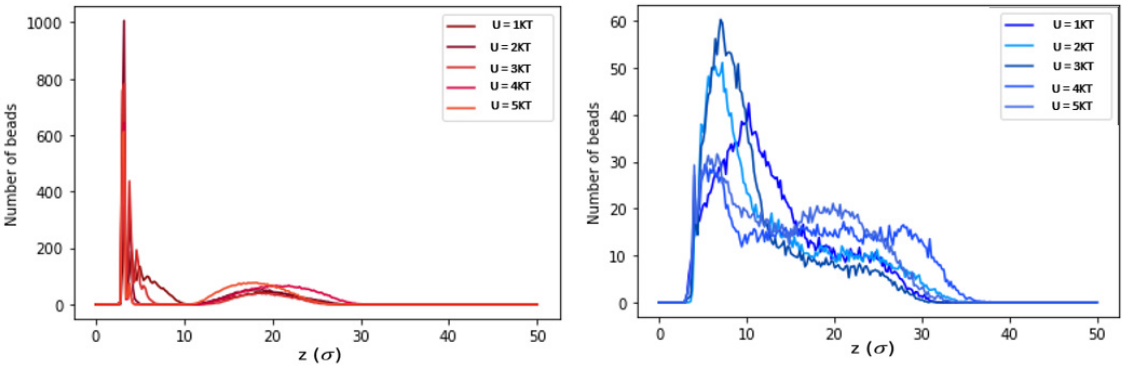

Figure 4.48: plots showing the number of red beads (left) and blue beads (right) above the surface for different strength of interactions in the system with tri-block co-polymers; the profiles have similarities with the ones in the previous system (Figure 4.30)

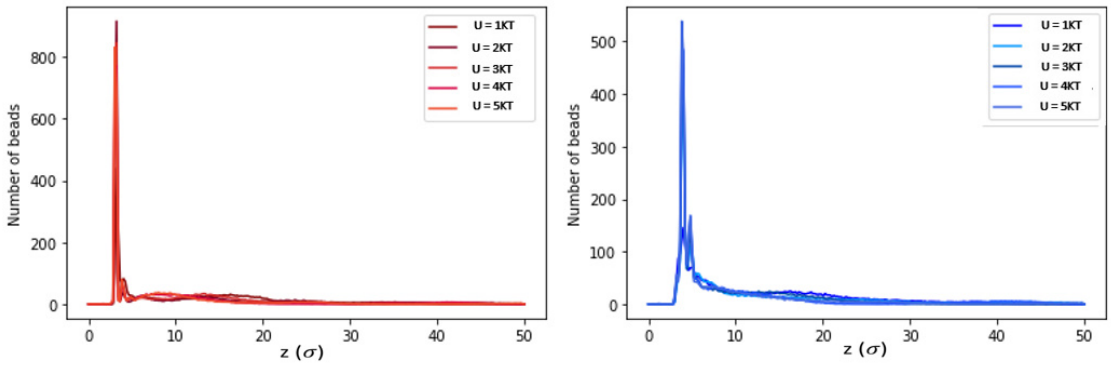

Figure 4.49: plots showing the number of red beads (left) and blue beads (right) above the surface for different strength of interactions in the system with random co-polymers; the profiles are different from the patterns in the previous system (Figure 4.36) in the way that most of the beads concentrate near the surface, also no peaks is visible in the middle.

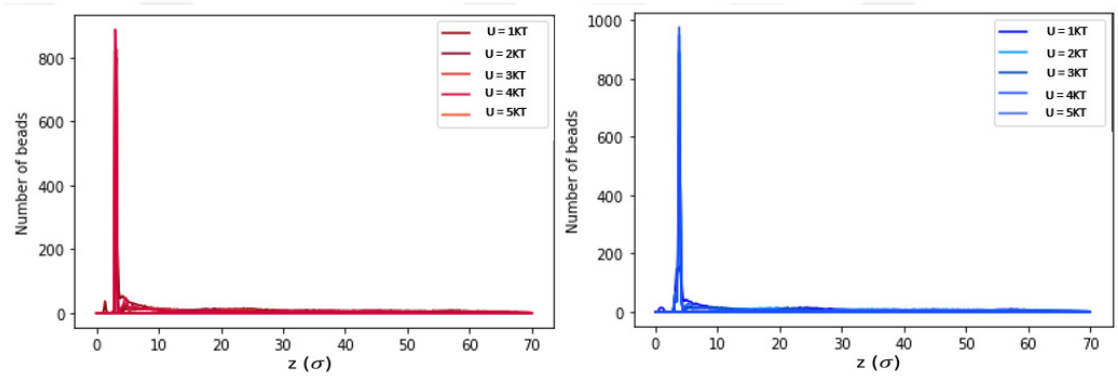

Figure 4.50: plots showing the number of red beads (left) and blue beads (right) above the surface for different strength of interactions in the system with alternating co-polymers

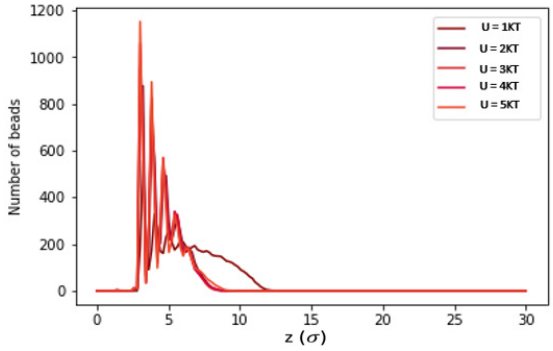

Figure 4.51: plots showing the number of red beads above the surface for different strength of interactions for the system with homopolymers; when the strength of attractions is $1KT$, the profile is very much similar to the previous system (Figure 4.42). However, when attractions increase, the pattern changes to sharp fluctuations near the surface. The patterns are still similar to the previous system in terms of having the beads concentrated near the surface.

5. Conclusion and Future prospects

Yet some of the simulations show the adsorption of co-polymers on the surface, we cannot declare that our goal of imitating adsorption process is perfectly achieved. The structural aspects of initial configurations, the dynamical features of the system components based on the defined interactions, as well as the lengths of simulation time fulfill our goals to do the project. However, the huge number of particles in our system and the compression of them in initial configurations may limit particle movements. Therefore, it may cause a restriction on the process to be carried out completely.

The strength of interactions defined inside the systems play a significant role in simulations. The more the strength of attractions are, the more beads gather near the surface. In this way, the accumulation of di-block co-polymers does not occur near the surface when the strength of attractions (between surface beads and red beads) is $3KT$. Moreover, the configurations with strength of attractions $5KT$, $10KT$, and $15KT$ lead to the red part of co-polymers placed on the surface, where the number of red beads gathering near the surface increase, respectively.

The population of the co-polymers can have effects on the concentration profile of the beads through the process. In the study, we tried two distinct number of co-polymer chains (256 and 144). In both systems, the extracted patterns for curves obey exponential and gaussian functions; however, the symmetry of the curves have differences. Since all the other factors remain the same for the systems, we can conclude that such processes (surface-adsorption of co-polymers) can be a collective behavior of the system, meaning assemblies of beads leads to dynamical behaviors which is not observed in individuals'.

The graphs of beads' concentration on the surface are modeled with mathematical functions. The curves fit on graphs are exponential functions for red beads and gaussian functions for blue beads, which are appropriate patterns. The values of parameters have

been specified in order to compare different systems with together. The graphs of total number of beads are also plotted that include signs of fluctuations in the patterns of concentrations.

The chemical correlations corresponding to polymers can have significant affects in the adsorption process. The parameters related to the process are measured for polymers with specific chemical correlations, and the key features of their dynamical behavior (emerge on the parameters) are noted in the result section.

We think that the quantitative parameters (e.g., loop formation, and co-polymer brush) measured through the study can shed light on more aspects of polymer dynamics and contribute to novel ideas of research projects in polymer science. Moreover, we predict the formation of bead aggregations suspended among other beads above the surface to be a potential subject for investigating the topology of polymers near surfaces or at the interfaces. Focusing on these unexpected structures appeared in the simulation box and quantifying their shapes, size, and dynamics can lead to new aspects of this study.

The possibility of knot formation in our systems is still under question. The method we utilized did not be appreciable for our systems. The dense population of moving beads does not allow to understand if the successive cross sections of beads are attributed to a single chain or not. Then, we could not say by sure that the cross sections contribute to knot creations. An important point here is that our systems do not necessarily possess all the features of the entangled polymer structures where knots can be created. The condition for a polymeric system to be entangled is the existence of very long chains and a big number of monomer blocks along the chain.

We think that one can alter different aspects of our system (e.g., topology of chains, and geometry of the surface) and add new features (e.g., charged co-polymers, and mobile surface) to the system in order to use it for simulating other phenomena. It would

also be the case to eliminate the challenges we faced during the study by making modifications in the current system. Co-polymers are being widely known in biological phenomena and material applications. Consequently, we anticipate this study being practical for further studies with biological or biotechnological perspectives.

Bibliography

1. Brigham, Christopher. “Biopolymers: Biodegradable alternatives to traditional plastics.” *Green chemistry.* Elsevier, (2018). 753-770.

2. Chiappini, Cristina, Donatella Romano, and Francesca Matteucci. “Oxygen, carbon and nitrogen evolution in galaxies.” *Monthly Notices of the Royal Astronomical Society* 339.1 (2003): 63-81.

3. Hasselquist, Sten, et al. “APOGEE Chemical Abundances of the Sagittarius Dwarf Galaxy.” *The Astrophysical Journal* 845.2 (2017): 162.

4. Lardo, C., et al. “Carbon and nitrogen abundances of individual stars in the Sculptor dwarf spheroidal galaxy.” *Astronomy & Astrophysics* 585 (2016): A70.

5. Deamer, David. *First life: Discovering the connections between stars, cells, and how life began.* Univ of California Press, (2012).

6. Schrijver, Karel, and Iris Schrijver. *Living with the Stars: How the Human Body is Connected to the Life Cycles of the Earth, the Planets, and the Stars*. Oxford University Press, USA, (2015).

7. Van Beilen, Jan B., and Yves Poirier. “Production of renewable polymers from crop plants.” *The Plant Journal* 54.4 (2008): 684-701.

8. Klemm, Dieter, et al. “Cellulose: fascinating biopolymer and sustainable raw material.” *Angewandte chemie international edition* 44.22 (2005): 3358-3393.

9. Mohite, Bhavna V., and Satish V. Patil. “A novel biomaterial: bacterial cellulose and its new era applications.” *Biotechnology and Applied Biochemistry* 61.2 (2014): 101-110.

10. Mohite, Bhavana V., and Satish V. Patil. “Impact of microbial cellulases on microbial cellulose biotechnology.” *New and Future Developments in Microbial Biotechnology and Bioengineering.* Elsevier, (2016). 31-40.

11. Gupta, Vijai Kumar, ed. *New and future developments in microbial biotechnology and bioengineering: Aspergillus system properties and applications.* Elsevier, (2016).

12. Richmond, Todd. “Higher plant cellulose synthases.” *Genome biology* 1.4 (2000): 1-5.

13. Kubicki, James D., et al. “The shape of native plant cellulose microfibrils.” *Scientific reports* 8.1 (2018): 1-8.

14. Hermans, P. H., and A. Weidinger. “X-ray studies on the crystallinity of cellulose.” *Journal of Polymer Science* 4.2 (1949): 135-144.

15. Heller, Iddo, et al. “Optical tweezers analysis of DNA–protein complexes.” *Chemical reviews* 114.6 (2014): 3087-3119.

16. Nixon, Conor A., et al. “Detection of propene in Titan’s stratosphere.” *The Astrophysical Journal Letters* 776.1 (2013): L14.

17. Wang, T., Yang, H., Kubicki, J. D. & Hong, M. Cellulose Structural Polymorphism in Plant Primary Cell Walls Investigated by HighField 2D Solid-State NMR Spectroscopy and Density Functional Teory Calculations. Biomacromolecules (2016).

18. Harris, D. M. et al. Cellulose microfibril crystallinity is reduced by mutating C-terminal transmembrane region residues CESA1A903V and CESA3T942I of cellulose synthase. Proceedings of the National Academy of Sciences 109, 4098–4103 (2012).

19. Lee, C. M., Kafe, K., Huang, S. & Kim, S. H. Multimodal broadband vibrational sum frequency generation (MM-BB-V-SFG) spectrometer and microscope. Te Journal of Physical Chemistry B 120, 102–116 (2015).

20. Rubinstein, Michael, and Ralph H. Colby. *Polymer physics.* Vol. 23. New York: Oxford university press, 2003.

21. H. J. Stern, in: Rubber Technology and Manufacture, 2nd edn, C. M. Blow and C. Hepburn (Eds.), pp. 1–20. Butterworths, London (1982).

22. S. T. Semegen, in: Rubber Technology, 2nd edn, M. Morton (Ed.), pp. 152–177. Van NostrandReinhold, New York, NY (1973).

23. P. C. Painter and M. M. Coleman, Fundamentals of Polymer Science. An Introductory Text, 2nd edn. Technomic, Lancaster, PA (1997).

24. Bower, D. (2002). Introduction. In *An Introduction to Polymer Physics* (pp. 1-26). Cambridge: Cambridge University Press. doi:10.1017/CBO9780511801280.002

25. Dorel Feldman (2008) Polymer History, Designed Monomers and Polymers, 11:1, 1-15, DOI: 10.1163/156855508X292383

26. Malerba, Massimo, and Raffaella Cerana. "Recent applications of chitin-and chitosan-based polymers in plants." *Polymers* 11.5 (2019): 839.

27. Mai, Y.; Eisenberg, A. Self-assembly of block copolymers. Chem. Soc. Rev. (2012), 41, 5969−5985.

28. Bates, F. S.; Fredrickson, G. H. Block copolymers: designer soft materials. Phys. Today (1999), 52, 32−38.

29. "Hermann Staudinger: Foundation of Polymer Science". National Historic Chemical Landmarks. American Chemical Society. Archived from the original on January 12, (2013).

30. Jonas, Rainer, and Luiz F. Farah. "Production and application of microbial cellulose." *Polymer degradation and stability* 59.1-3 (1998): 101-106.

31. Fiedler, S., Fiissel, M. and Sattler, K., Zentrulbl. Microbiof., (1989), 144, 473

32. Xu, Zhongde, et al. "Structure/chain-flexibility relationships of polymers." *Physical Properties of Polymers* (1995): 1-50.

33. Winter, Horst Henning. “The occurrence of self-similar relaxation in polymers.” *Journal of non-crystalline solids* 172 (1994): 1158-1167.

34. Kruteva, Margarita, et al. “Self-similar polymer ring conformations based on elementary loops: A direct observation by SANS.” *ACS Macro Letters* 9.4 (2020): 507-511.

35. Nahum, Adam. “Universality class of the two-dimensional polymer collapse transition.” Phys. Rev. E 93, 052502 (May 2016). ®2016 American Physical Society

36. Klein, D. J., and W. A. Seitz. “Self-similar self-avoiding structures: Models for polymers.” *Proceedings of the National Academy of Sciences* 80.10 (1983): 3125-3128.

37. Peitgen, Heinz-Otto, et al. *Chaos and fractals: new frontiers of science.* Vol. 7. New York: Springer, (1992).

38. Brostow, Witold, et al. “Flexibility of polymers defined and related to dynamic friction.” *J. Mater. Sci. Res* 8.3 (2019): 31-35.

39. Mao, Shifan, et al. “Impact of conformational and chemical correlations on microphase segregation in random copolymers.” *Macromolecules* 49.11 (2016): 4358-4368.

40. Houdayer, J.; Müller, M. Phase diagram of random copolymer melts: a computer simulation study. Macromolecules (2004), 37, 4283− 4295.

41. Slimani, Mohammed Zakaria, et al. “Dynamic heterogeneity in random and gradient copolymers: A computational investigation.” Macromolecules 46.12 (2013): 5066-5079.

42. Kittel, Charles, Paul McEuen, and Paul McEuen. *Introduction to solid state physics.* Vol. 8. New York: Wiley, (1996).

43. Bajpai, Gaurav, et al. “Mesoscale phase separation of chromatin in the nucleus.” *Elife* 10 (2021): e63976.

44. Fredrickson, G. H.; Milner, S. T.; Leibler, L. Multicritical phenomena and microphase ordering in random block copolymers melts. Macromolecules (1992), 25, 6341−6354

45. Adams, J. B. Bonding Energy Models. Encyclopedia of Materials: Science and Technology 763–767 (2001) doi:10.1016/B0-08-043152-6/00146-7.

46. On the determination of molecular fields. —II. From the equation of state of a gas. Proceedings of the Royal Society of London. Series A, Containing Papers of a Mathematical and Physical Character 106, 463–477 (1924).

47. Schleif, Robert. "DNA looping." *Annual review of biochemistry* 61.1 (1992): 199-223.

48. Rippe, Karsten. "Making contacts on a nucleic acid polymer." *Trends in biochemical sciences* 26.12 (2001): 733-740.

49. Jun, Suckjoon, and John Bechhoefer. "Role of polymer loops in DNA replication." *arXiv preprint physics/0306156* (2003).

50. Alberts, Bruce, Dennis Bray, Julian Lewis, Martin Raff, Keith Roberts, and James D. Watson. "Molecular Biology of the Cell 3E." (1994).

51. Mashaghi, Alireza, Roeland J. van Wijk, and Sander J. Tans. "Circuit topology of proteins and nucleic acids." Structure 22.9 (2014): 1227-1237.

52. Kremer, K. & Grest, G. S. Dynamics of entangled linear polymer melts: A molecular-dynamics simulation. The Journal of Chemical Physics 92, 5057 (1998).

53. Grest, Gary S., and Kurt Kremer. "Molecular dynamics simulation for polymers in the presence of a heat bath." *Physical Review A* 33.5 (1986): 3628.

54. Sides, Scott W., Gary S. Grest, and Mark J. Stevens. "Large-scale simulation of adhesion dynamics for end-grafted polymers." *Macromolecules* 35.2 (2002): 566-573.

55. Grest, Gary S., Kurt Kremer, and T. A. Witten. "Structure of many arm star polymers: a molecular dynamics simulation." *Macromolecules* 20.6 (1987): 1376-1383.

56. Grest, Gary S. “Structure of many-arm star polymers in solvents of varying quality: A molecular dynamics study.” *Macromolecules* 27.13 (1994): 3493-3500.

57. Steinhauser, Martin Oliver. “A molecular dynamics study on universal properties of polymer chains in different solvent qualities. Part I. A review of linear chain properties.” *The Journal of chemical physics* 122.9 (2005): 094901

58. Wang, Xipeng, et al. “The Lennard-Jones potential: when (not) to use it.” *Physical Chemistry Chemical Physics* 22.19 (2020): 10624-10633.

59. Plimpton, Steve. “Fast parallel algorithms for short-range molecular dynamics.” *Journal of computational physics* 117.1 (1995): 1-19.

60. Humphrey, William, Andrew Dalke, and Klaus Schulten. “VMD: visual molecular dynamics.” *Journal of molecular graphics* 14.1 (1996): 33-38.

61. Stukowski, Alexander. “Visualization and analysis of atomistic simulation data with OVITO–the Open Visualization Tool.” *Modelling and simulation in materials science and engineering* 18.1 (2009): 015012.

62. Harris, Charles R., et al. “Array programming with NumPy.” *Nature* 585.7825 (2020): 357-362.

63. McKinney, W., & others. (2010). Data structures for statistical computing in python. In *Proceedings of the 9th Python in Science Conference* (Vol. 445, pp. 51–56).

64. J. D. Hunter, “Matplotlib: A 2D Graphics Environment”, Computing in Science & Engineering, vol. 9, no. 3, pp. 90-95, (2007).

65. Kamalov, Timur F. “Physics of Non-Inertial Reference Frames.” *AIP Conference Proceedings.* Vol. 1316. No. 1. American Institute of Physics, (2010).

66. Drivotin, Oleg Igorevich. “Reference frames in classical and relativistic physics.” *arXiv preprint arXiv:1403.1787* (2014).

67. Adhikari, Basudam, and Sarmishtha Majumdar. “Polymers in sensor applications.” *Progress in polymer science* 29.7 (2004): 699-766.

68. E. Pludeman and N. Collins, Adhesion Science and Technology, Vol. 9a, Plenum Press, New York, (1975).

69. P. O. Brown and D. Botstein, Nature Genetics Supplement, (1999), 21.

70. J. K. Cox, A. Eisenberg and R. B. Lennox, Curr. Opin. Colloid Interface Sci., (1999), 4.

71. 71. Young, Robert J., and Peter A. Lovell. *Introduction to polymers*. CRC press, 2011.

72. Stokes, Robert J., and D. Fennell Evans. *Fundamentals of interfacial engineering.* John Wiley & Sons, 1996.

73. Fleer, Gerard, et al. *Polymers at interfaces.* Springer Science & Business Media, (1993).

74. Gurevitch, Inna, and Simcha Srebnik. “Conformational behavior of polymers adsorbed on nanotubes.” *The Journal of chemical physics* 128.14 (2008): 144901.

Appendix

The codes used in the study are available at https://github.com/SDaryakp/pt.git.